TFAWS Interdisciplinary Paper Session

Thermal Analysis for the SRTMV-N2 Plume Impingement Test Panel (PITP)

Presented by
Vincent Cuda
AMA/NASA LaRC

Thermal & Fluids Analysis Workshop
TFAWS 2014
August 4 - 8, 2014
NASA Glenn Research Center
Cleveland, OH

OUTLINE

- Objectives
- Instrumentation
- Motor Test
- Data Processing & Thermal Analysis
- Key Observations

Objectives for PITP Risk Mitigation Task

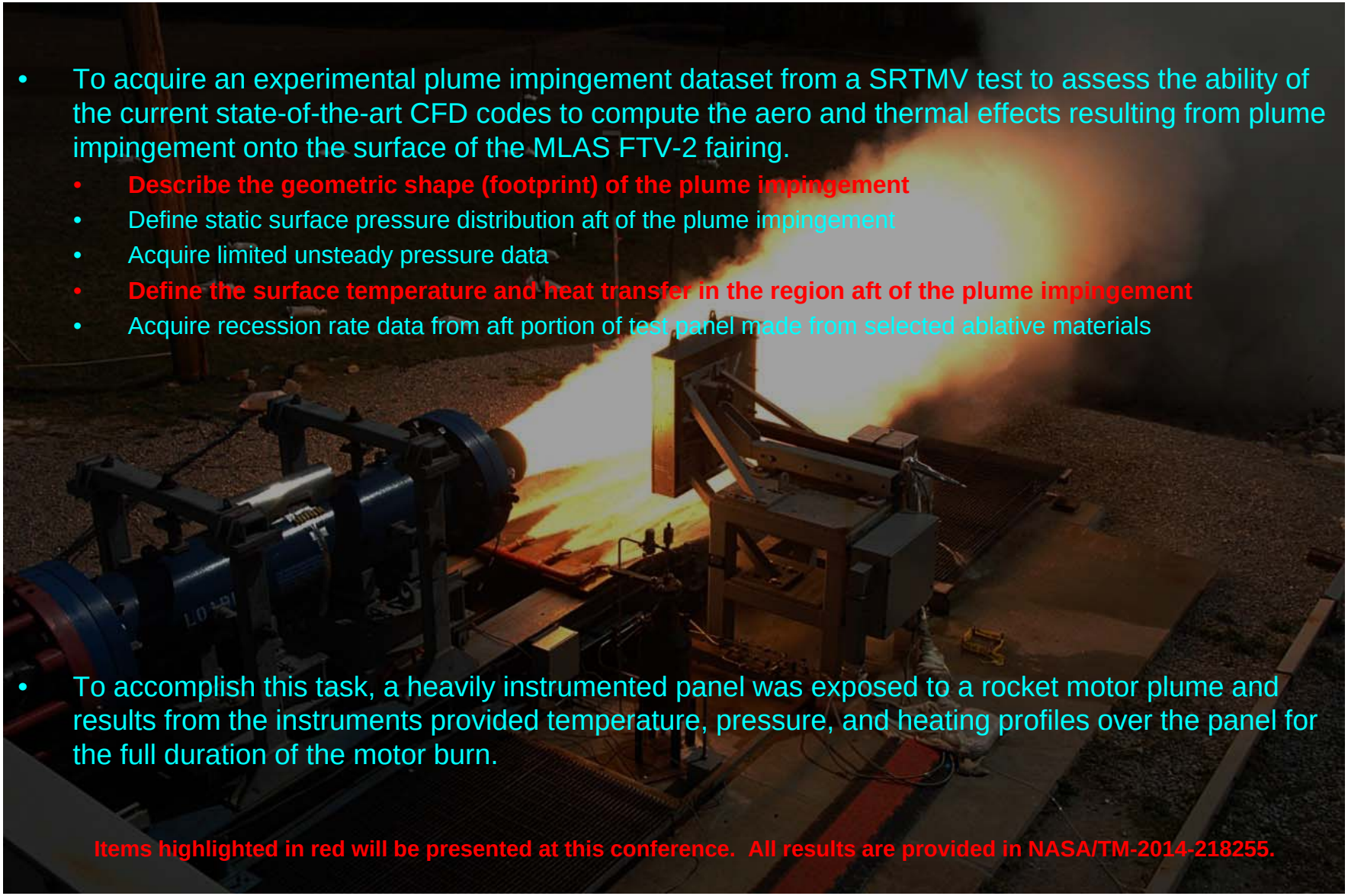

- To acquire an experimental plume impingement dataset from a SRTMV test to assess the ability of the current state-of-the-art CFD codes to compute the aero and thermal effects resulting from plume impingement onto the surface of the MLAS FTV-2 fairing.
  - **Describe the geometric shape (footprint) of the plume impingement**
  - Define static surface pressure distribution aft of the plume impingement
  - Acquire limited unsteady pressure data
  - **Define the surface temperature and heat transfer in the region aft of the plume impingement**
  - Acquire recession rate data from aft portion of test panel made from selected ablative materials

- To accomplish this task, a heavily instrumented panel was exposed to a rocket motor plume and results from the instruments provided temperature, pressure, and heating profiles over the panel for the full duration of the motor burn.

Items highlighted in red will be presented at this conference. All results are provided in NASA/TM-2014-218255.

Team Membership

Research Team Members	Responsibility
David Witte (LaRC)*	FTV-2 Aero Lead / PITP PM
Jeremy Pinier (LaRC)*	FTV-2 Deputy Aero Lead
Jason Mishtawy (MSFC)*	Research Lead
Jeremy Kenny (MSFC)*	Test Guidance/Dynamic Pressure Data
Vincent Cuda (LaRC)*	Thermal Analysis / Instrumentation
Bud Smith (MSFC)	Aerothermal Loads
Francisco Canabal (MSFC)	CFD (Loci CHEM)
Erik Tyler (LaRC)	CFD (USM3D)
Tom Jentink (LaRC)	CFD (VULCAN)
Ali Reza Mazaheri (LaRC)	CFD (Loci CHEM)
Rick Thompson (LaRC)	CFD Guidance
Darrel Davis (MSFC)	TPS Research
Stan Bouslog (JSC)	TPS Research
Scott Coughlin (JSC)	TPS Research
Molly White (JSC)	MPCV Plume Impingement
Brandon Oliver (JSC)	MPCV Plume Impingement

Acknowledgments	Role
Sam Yunis(LaRC)	Structural Dynamics Support
Sandy Webb (LaRC)	Mechanical Design
Dave Castle (LaRC)	Mechanical Stress Analysis
Tom Hall (LaRC)	Instrumentation Installation Lead
Wayne Geouge (LaRC)	Instrumentation Installation
Rick Irby (LaRC)	Instrumentation Support Systems
Jeff Petty (LaRC)	Pressure Scanner DAS
Dennis Strickland (MSFC)	SPTA Facility Manager
Jason Elmore (MSFC)	SPTA Data Acquistion
Ernie Wooten (MSFC)	SPTA Instrumentation
Scott Ringel (MSFC)	SRTMV-N2 Design Lead
Darrell Gaddy (MSFC)	IR Cameras

***Names in red are contributors to NASA/TM-2014-218255**

Instrumentation

PITP Planform View for the SRTMV-N2 Test

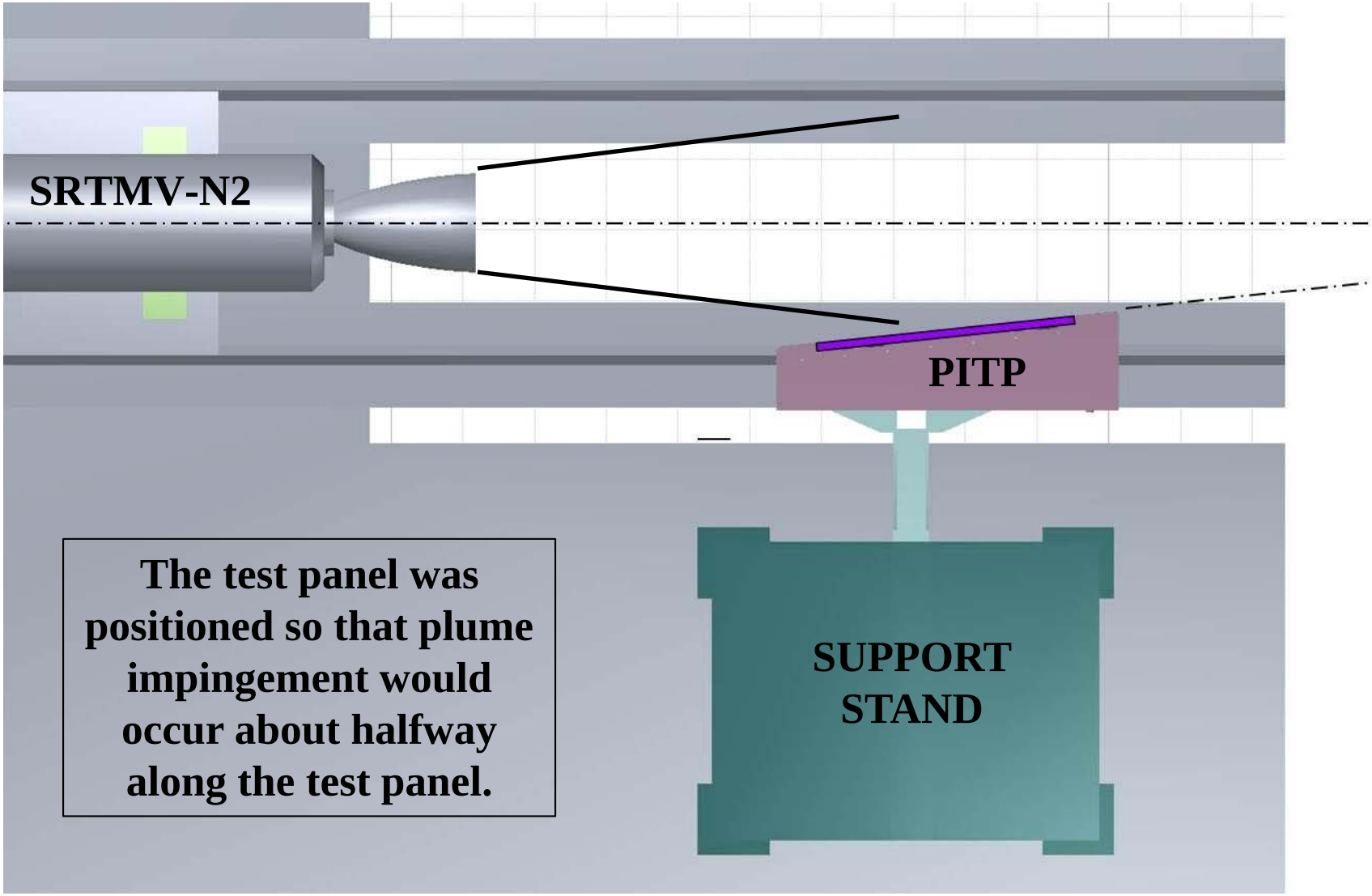

The test panel was positioned so that plume impingement would occur about halfway along the test panel.

Pre-test CFD Predictions

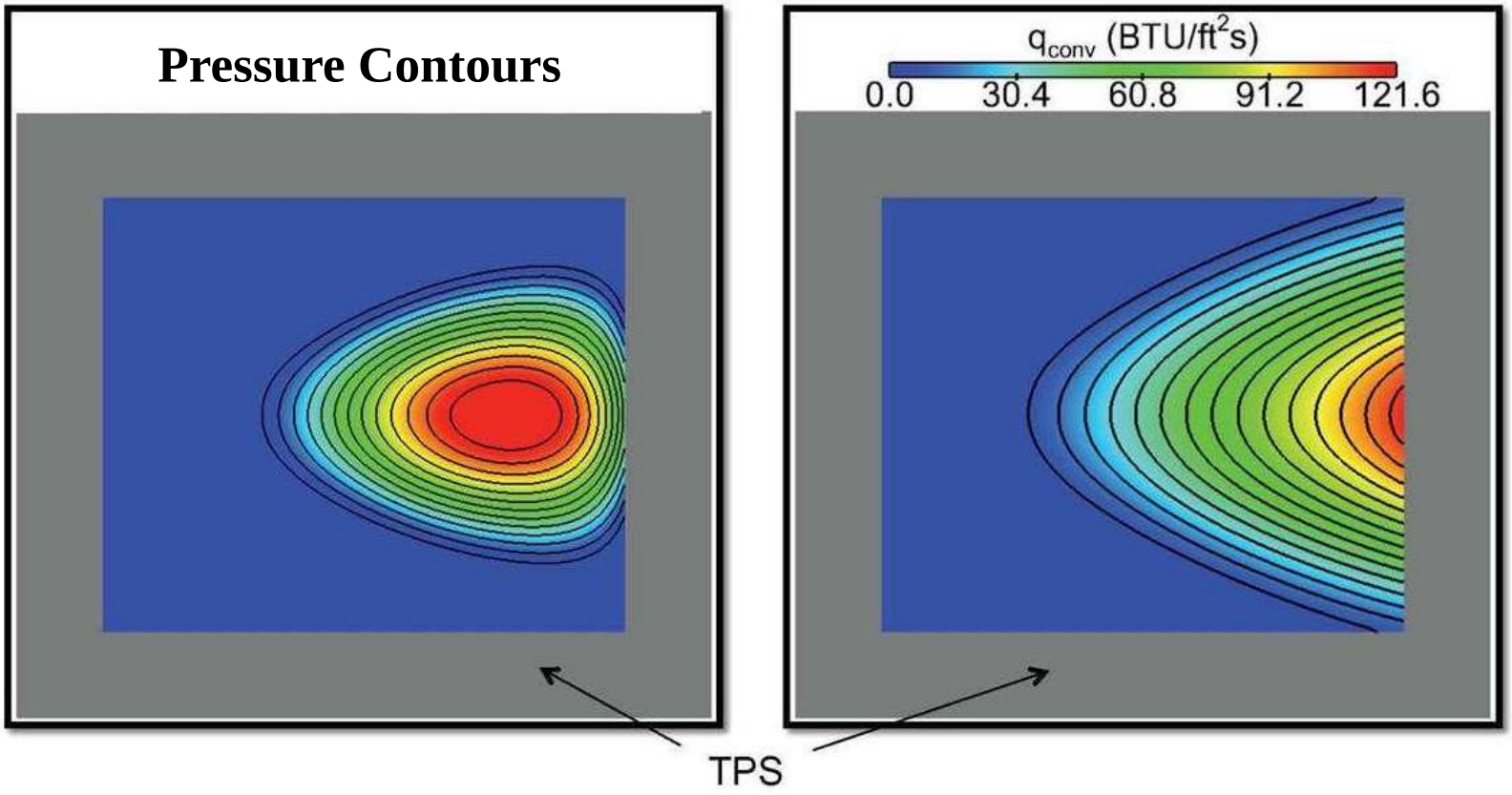

Loci-CHEM used to model the plume. Predictions provided estimates for the pressure and thermal loads. These results were used for instrument selection (type and range) and sensor placement.

Thermal Instruments

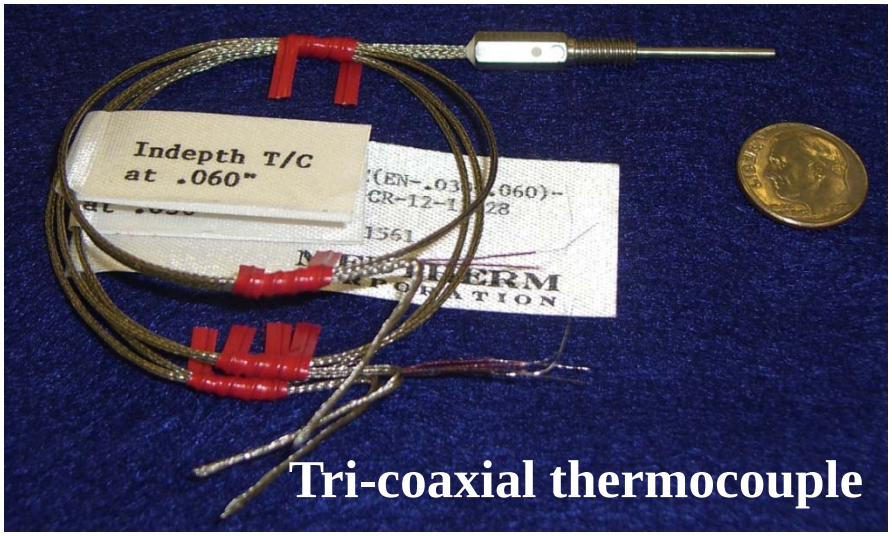

Tri-coaxial thermocouple

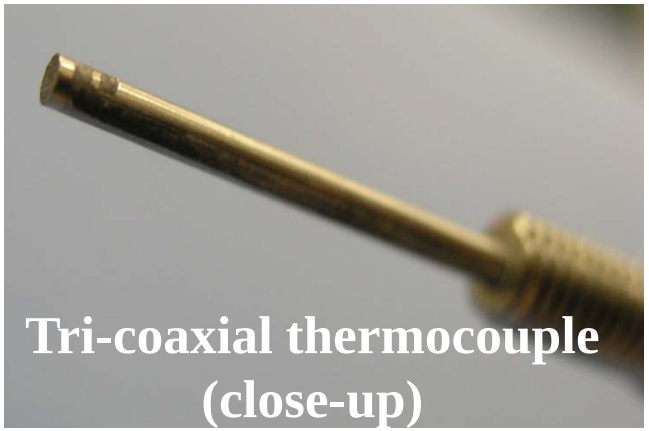

Tri-coaxial thermocouple (close-up)

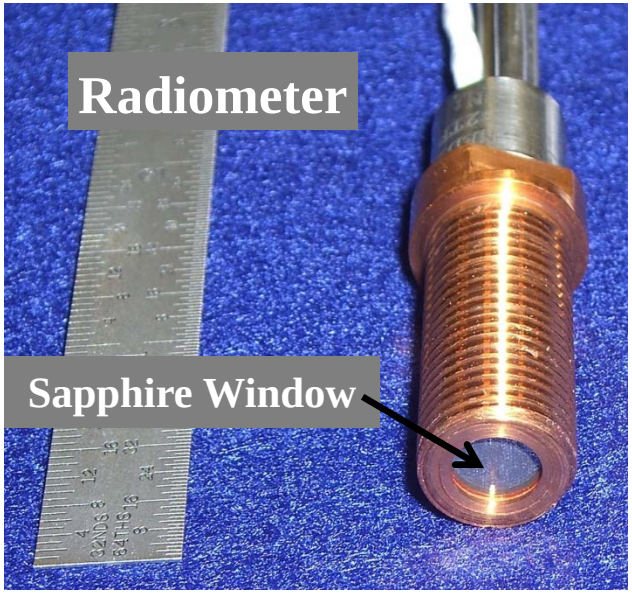

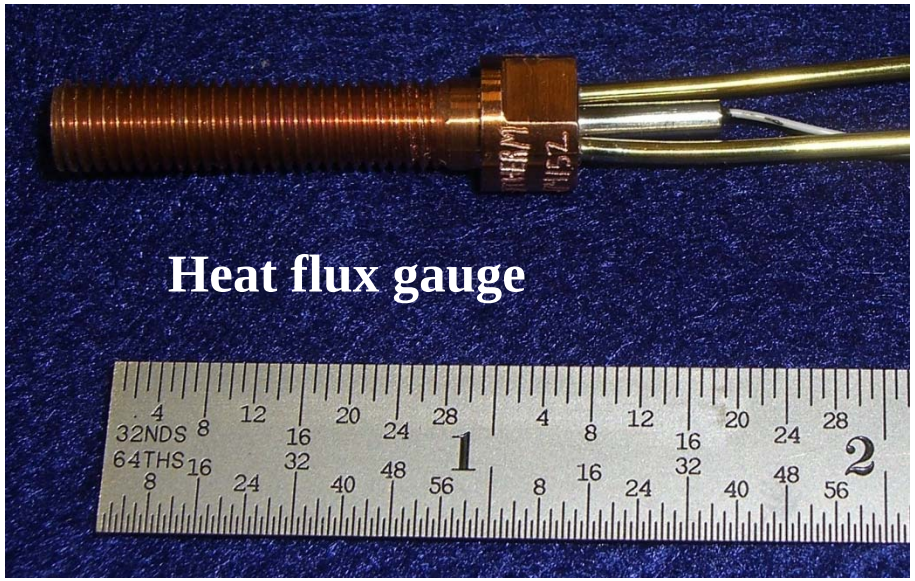

Heat flux gauge

Instrument Suite Summary

- **Direct Measurements**
  - Gardon Gauges (9)
  - Schmidt-Boelter Gauges (3)
  - Radiometers (4)

- **Indirect Measurement**
  - Heat conduction via tri-coaxial thermocouple probe (3)
  - Analytical method using surface thermocouple measurements (46)

Instrument Layout

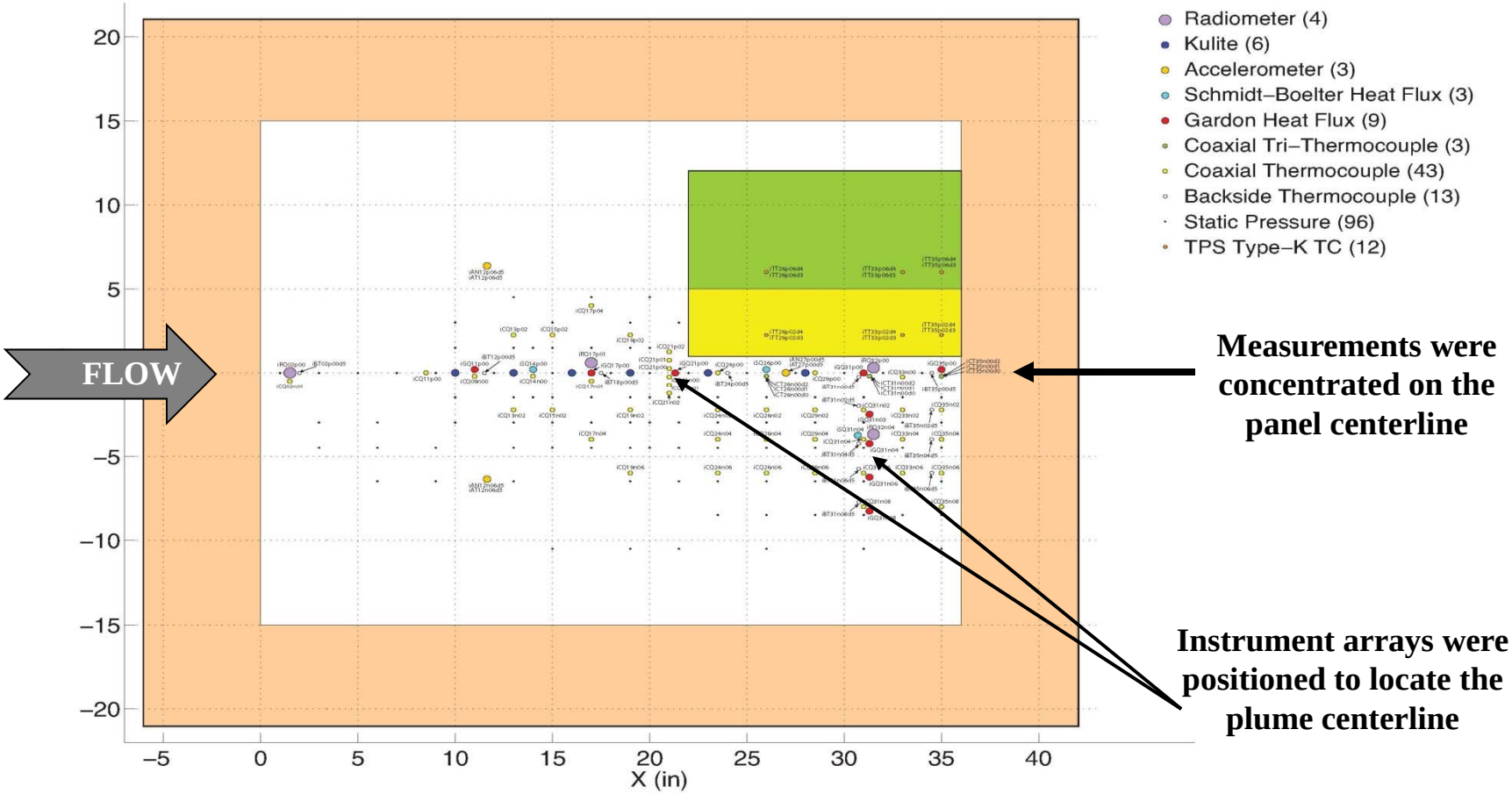

The instrument suite included 87 thermal measurements which provided a unique opportunity to estimate heat flux at coincident locations using a variety of instrument types and analytical methods.

Instrument Installation

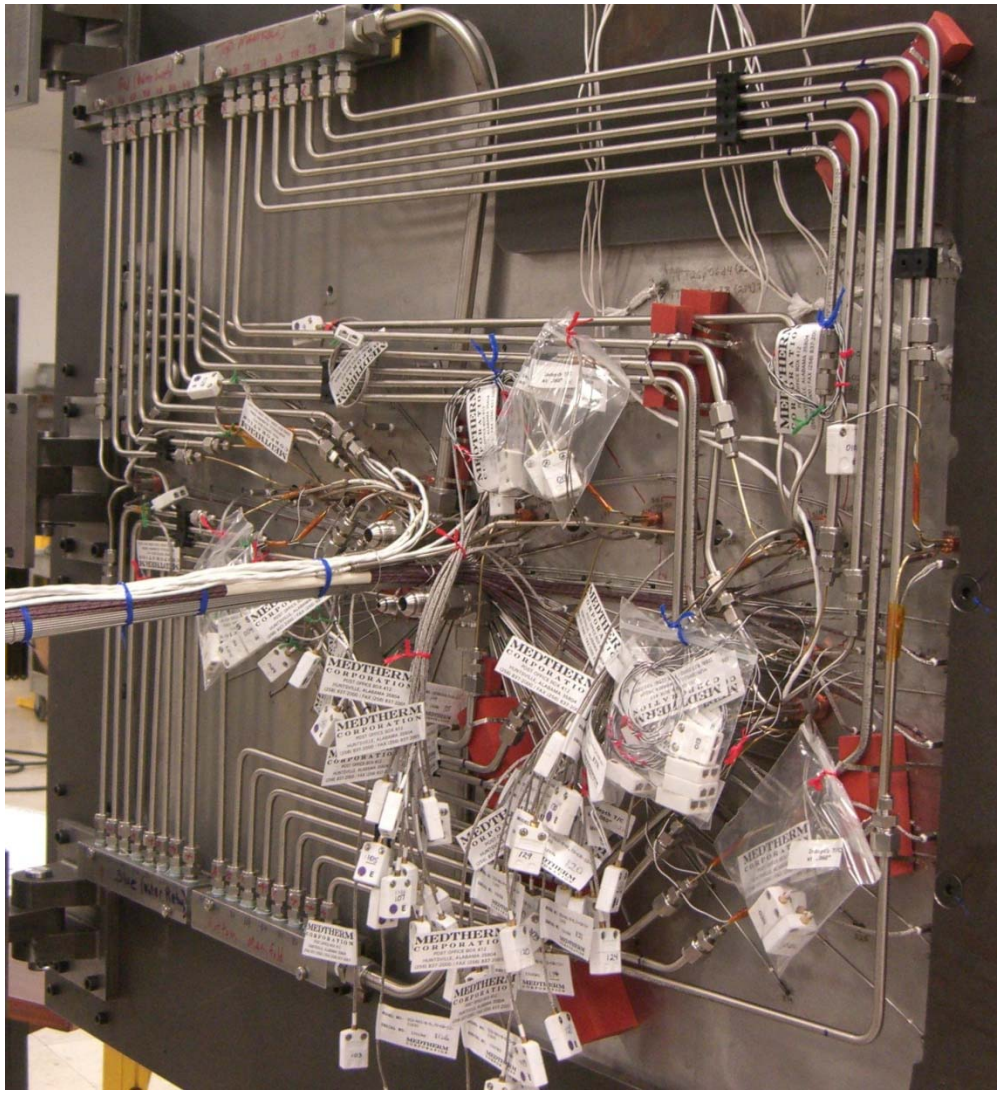

PITP Installation/Alignment Photos

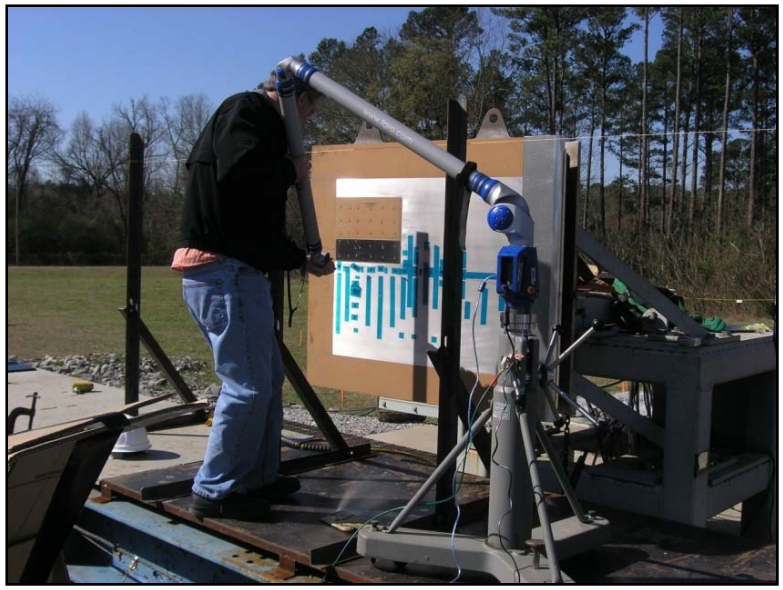

SRTMV-N2 PITP Test Video

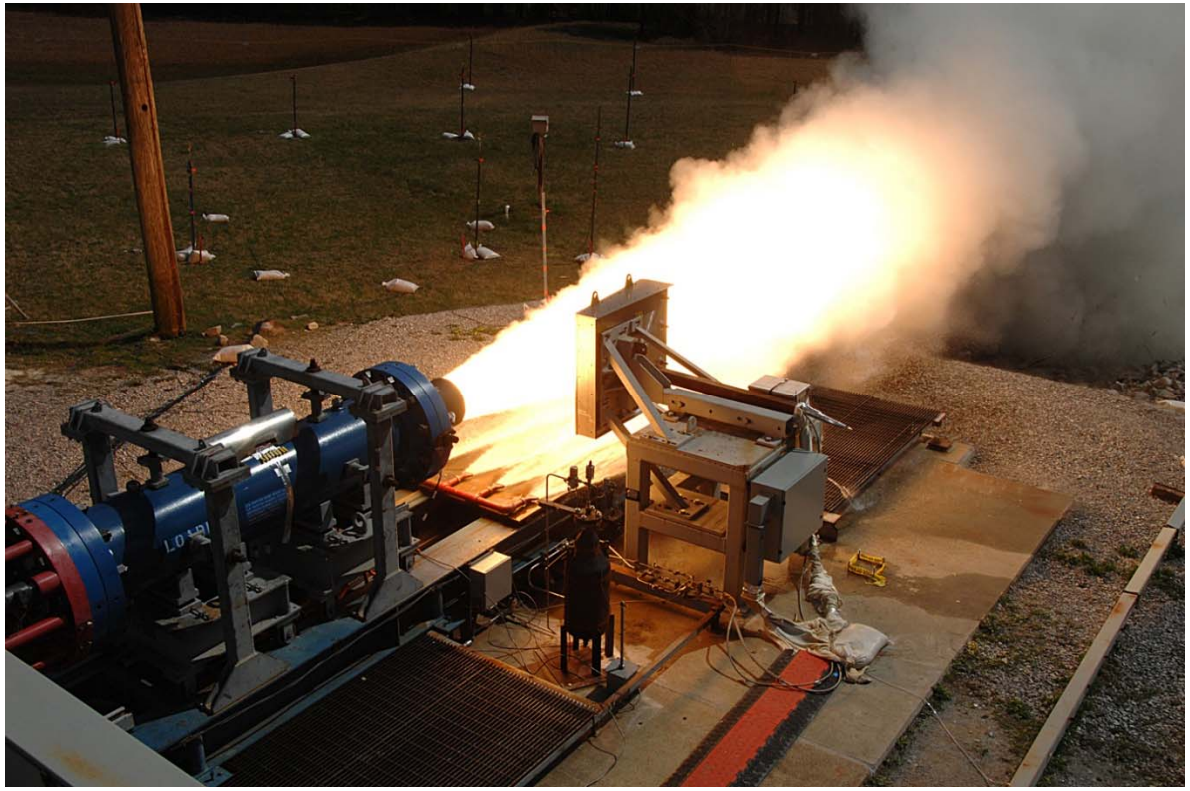

PB114-N2-HDvideo-3-alt2.avi

Timeline

Event	Test Clock [seconds]	Event Time [seconds]
Motor start	28.473	0.000
1st Steady State Period Begins	29.473	1.000
1st Steady State Period Ends	31.473	3.000
2nd Steady State Period Begins	36.473	8.000
2nd Steady State Period Ends	46.473	18.000
Motor burnout Begins	47.500	19.027
Motor burnout Ends	50.700	22.227

Time-averaged results herein were evaluated during the first steady state period.

Test Panel – Before and After

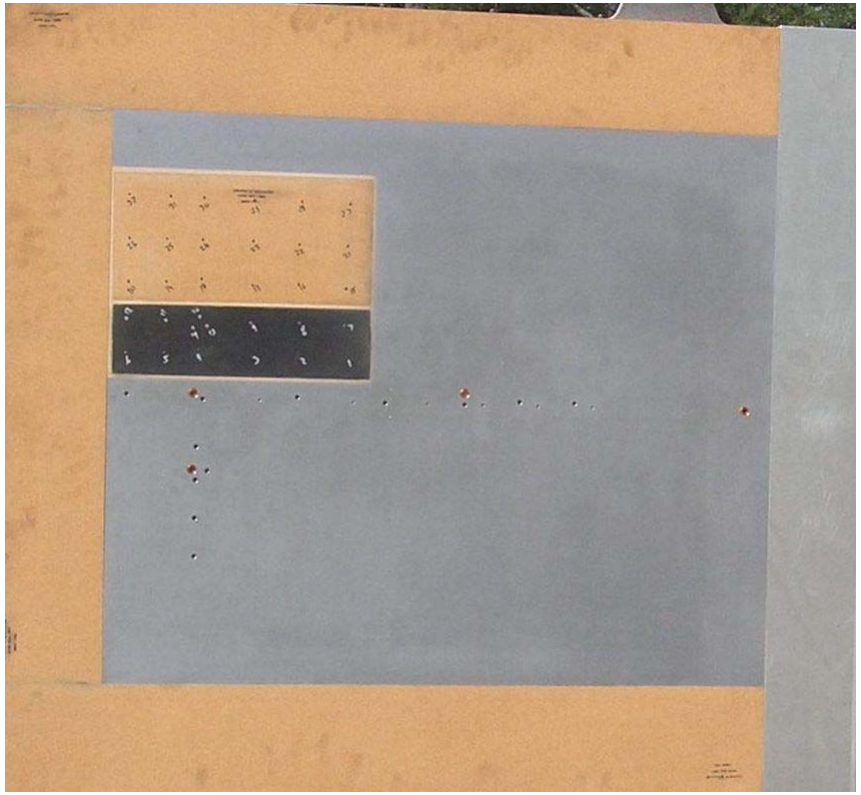

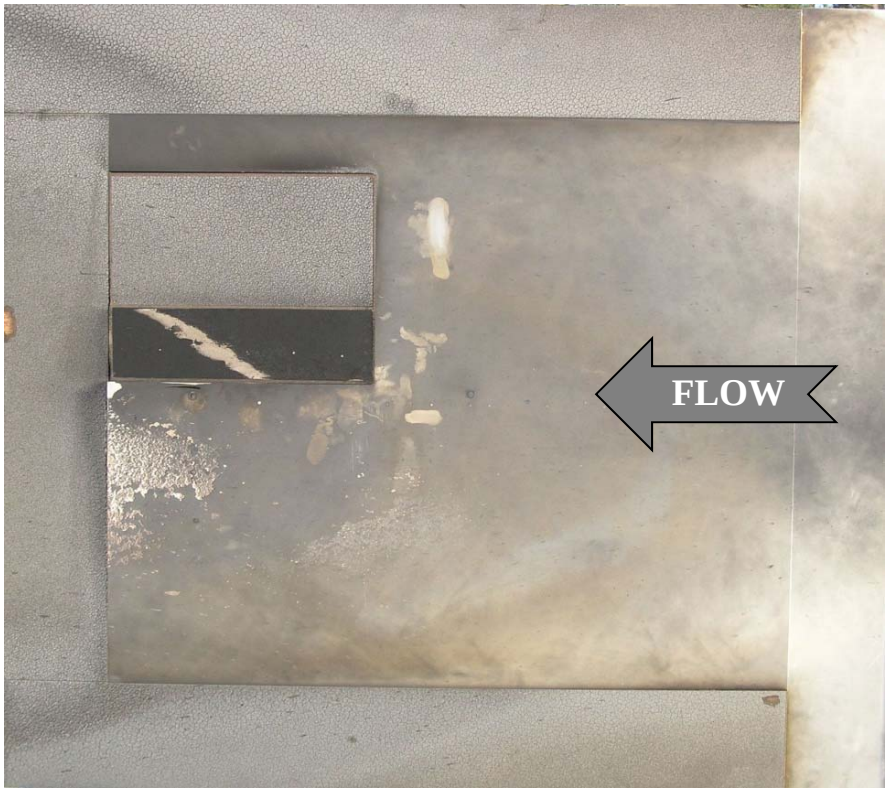

Post-test examination of the panel revealed significant recession of both the P-50 cork and VAMAC thermal protection materials. Aluminum deposition occurred below the plate centerline near the back end of the panel.

Test Panel – Aluminum Deposition

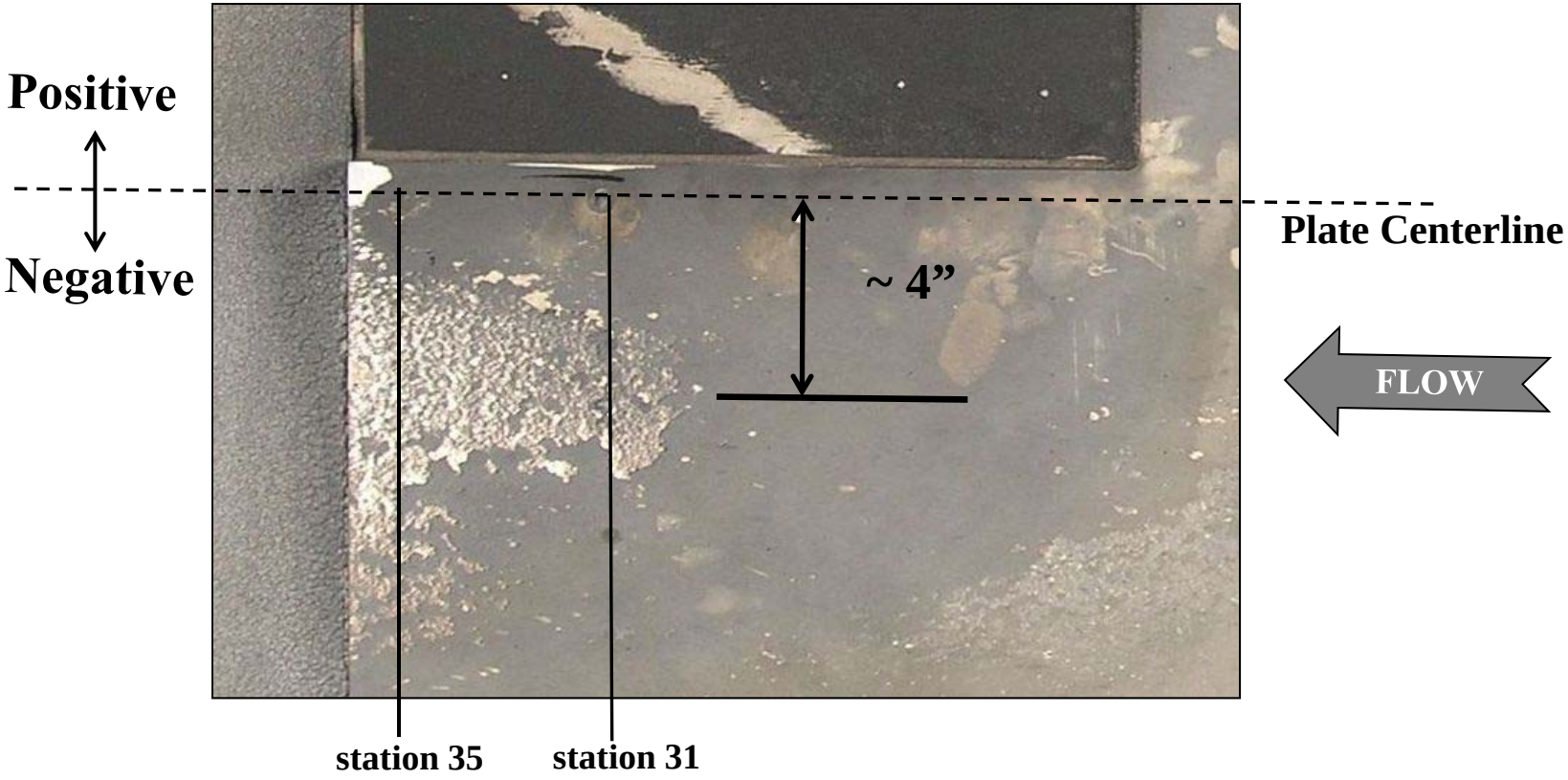

Aluminum deposition was heaviest for the last six inches of the panel. Instruments located at axial station 31 and beyond experienced elevated readings due to contact with molten aluminum.

Test Panel Burn Pattern
(contrast adjusted image)

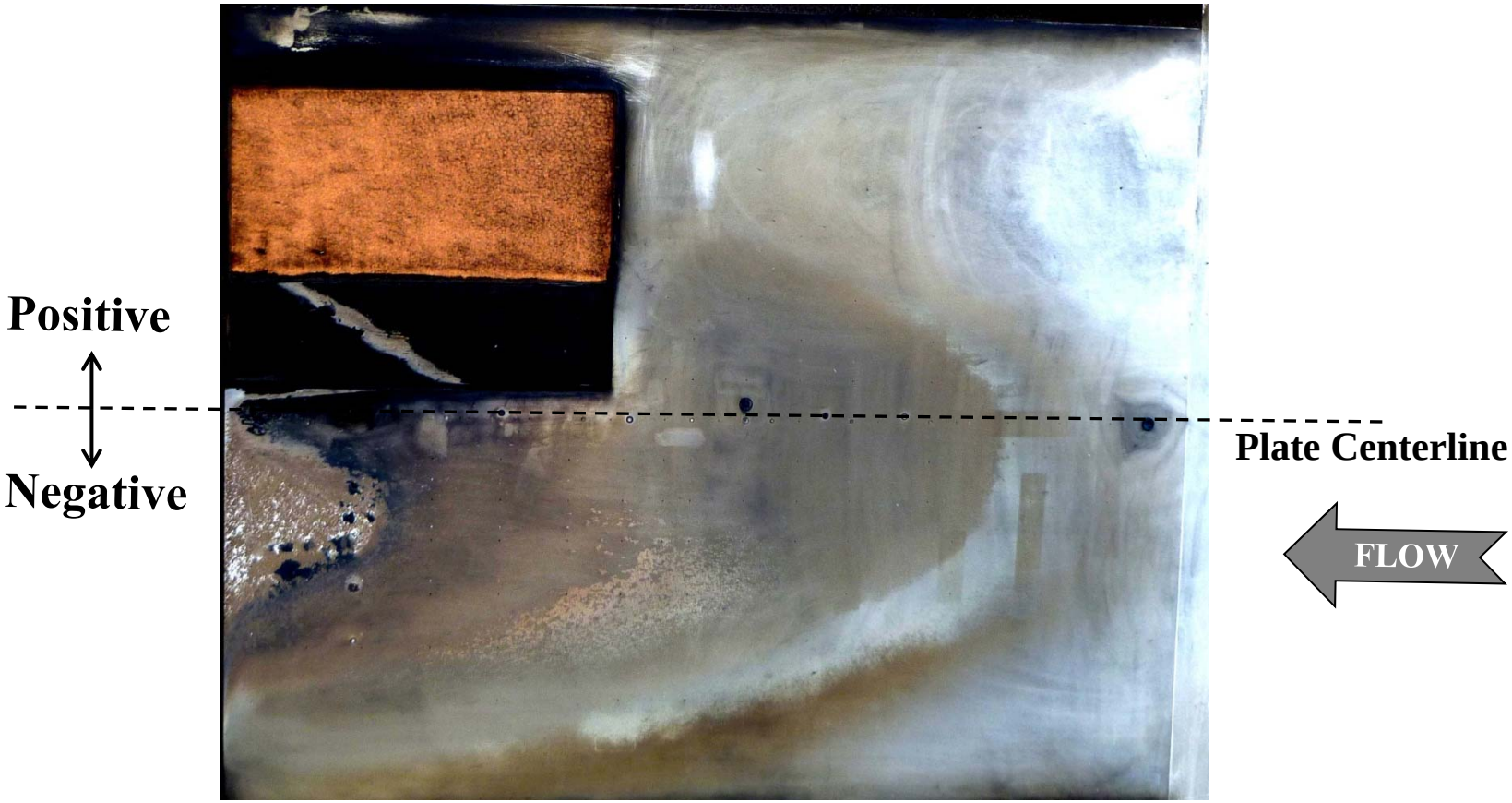

The motor exhaust plume produced a burn pattern that was offset (downward) from the plate centerline.

Data Processing and Thermal Analysis

Instrument Performance

- **Data Sampling**
  - All thermal data was taken at 2500 Hz.
  - A 100 Hz filter was applied at the data acquisition Center.
  - Test data was further smoothed out with a 25 point forward averaging routine.
  - Test results in this presentation are plotted at 10 Hz.

- **Instrument Inspection and data analysis revealed that:**
  - Five thermocouples failed during the test.
  - Six total heat flux gauges exceeded their design range for a portion of the test.
  - All radiometers exceeded their measurement range at the start of the test.

Centerline Temperature
(Coaxial & Tri-coaxial Thermocouples)

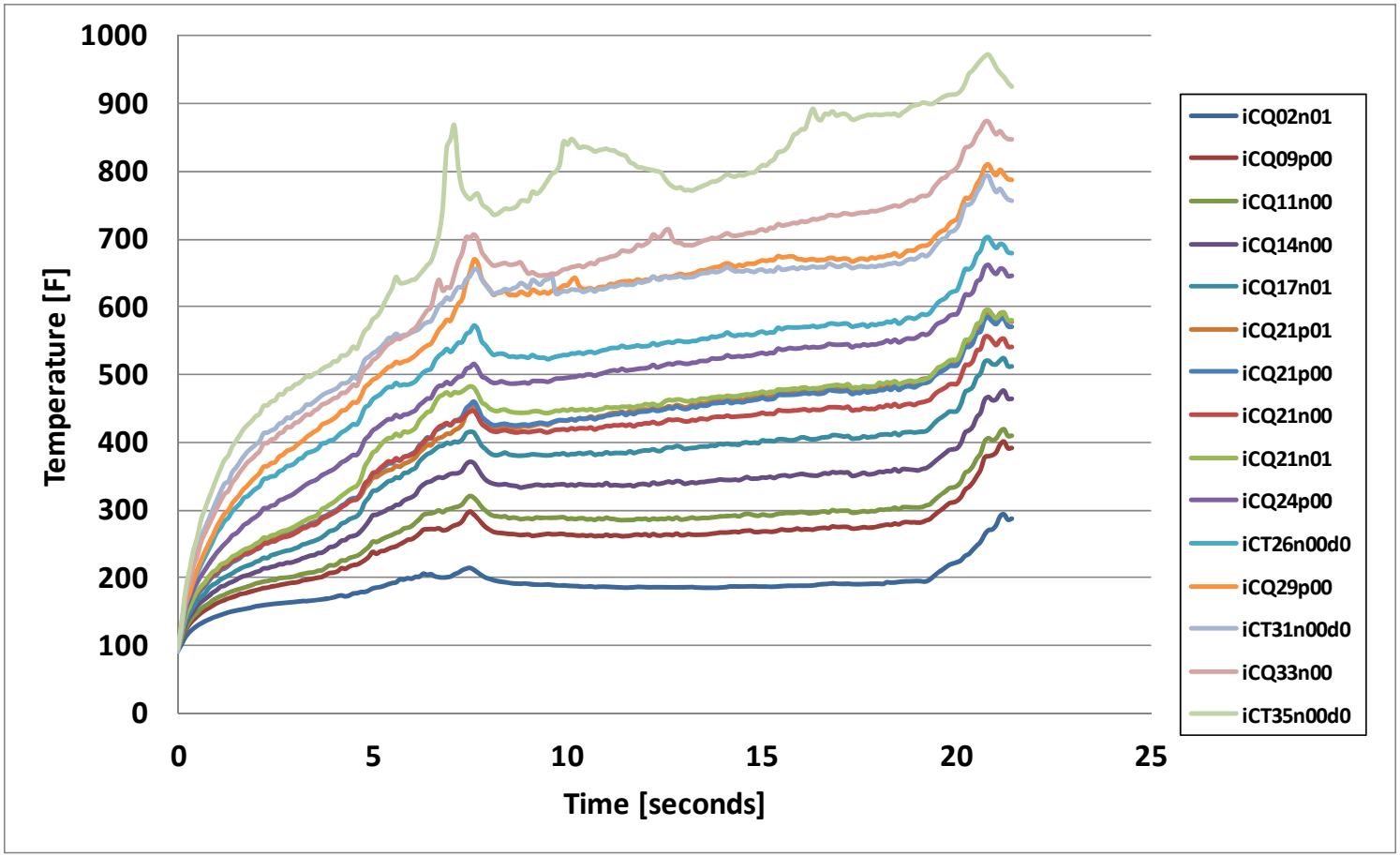

Due to the position of the plate, higher temperatures were predicted for the rear portion of the plate. Measurements supported this trend.

Spanwise Temperature
(Thermocouple Array - station 21)

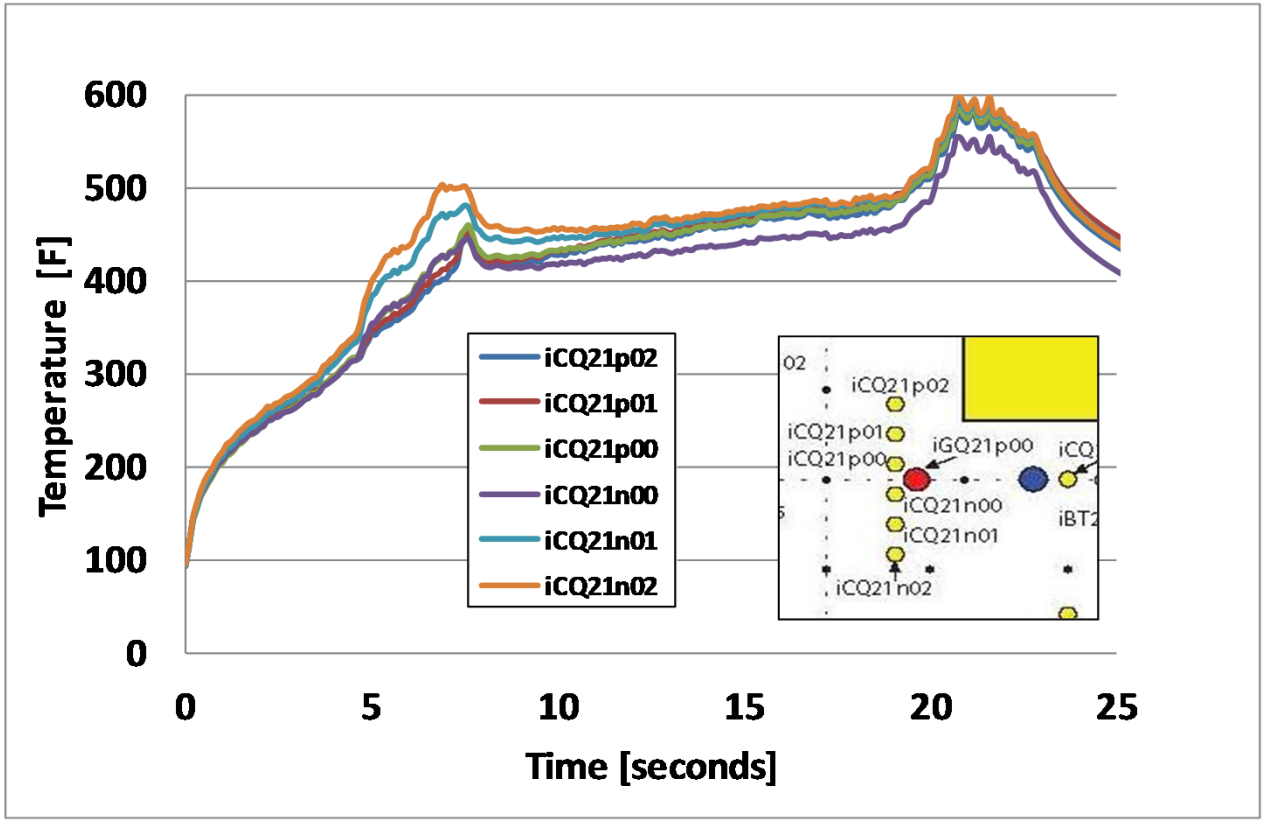

Initial thermocouple readings showed almost no bias during motor start-up. During the "transient event" temperature profiles departed from expected trends with the highest reading coming from thermocouple iCQ21n02. This suggests that the plume centerline was at least 1.00-1.25 inches or greater below the test panel centerline. After the transient event, the temperature rise rates for the thermocouples were nominally similar.

Centerline Heat Flux (Cold Wall)
(Gardon & Schmidt-Boelter Gauges)

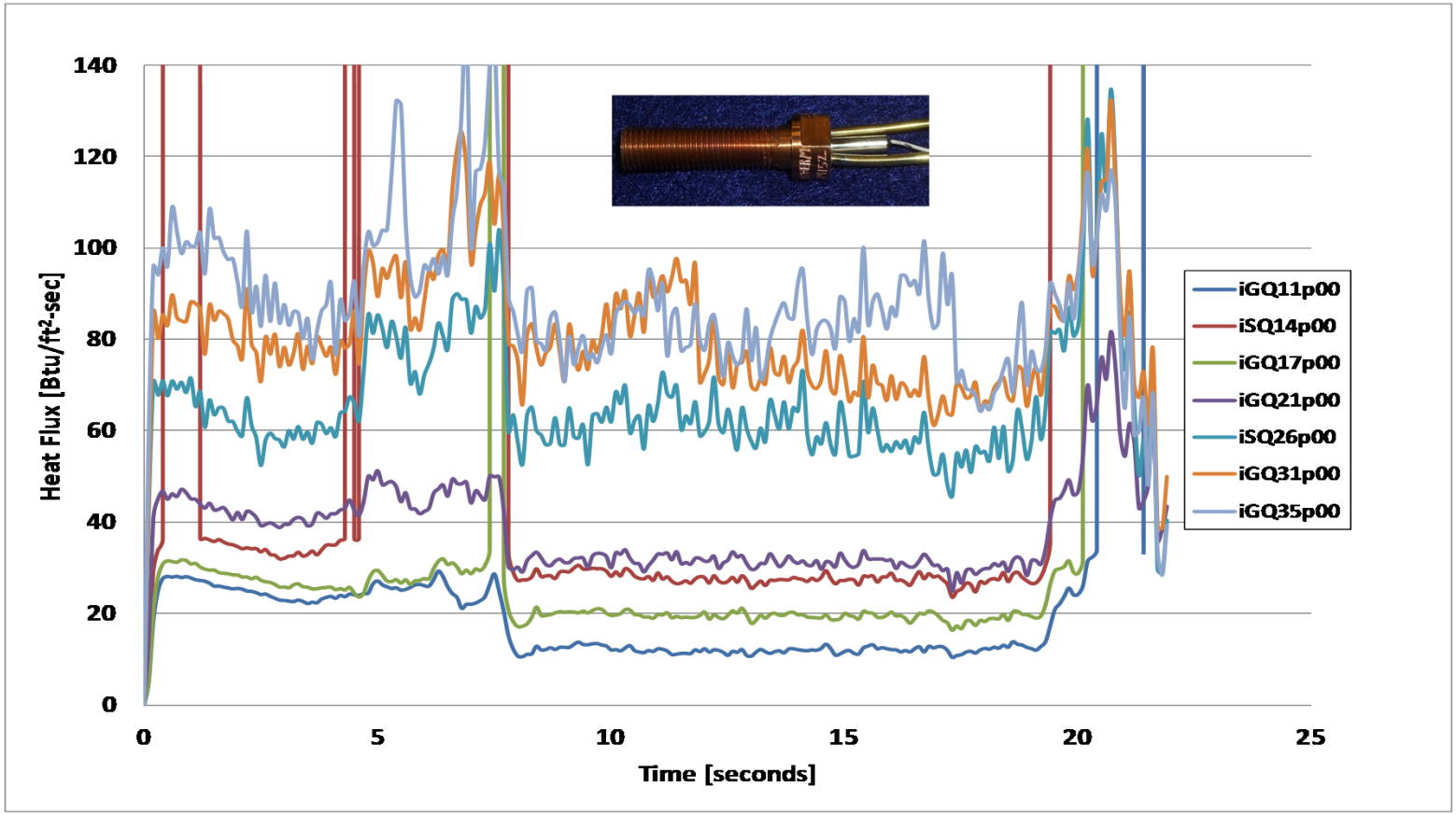

Due to the position of the plate, higher heat fluxes were predicted for the rear portion of the plate. Measurements agreed with predictions.
Schmidt-Boelter gauge (station 14) provided unexpected elevated readings.

Spanwise Heat Flux (Cold Wall)
(Gardon Gauge Heat Flux Array - station 31)

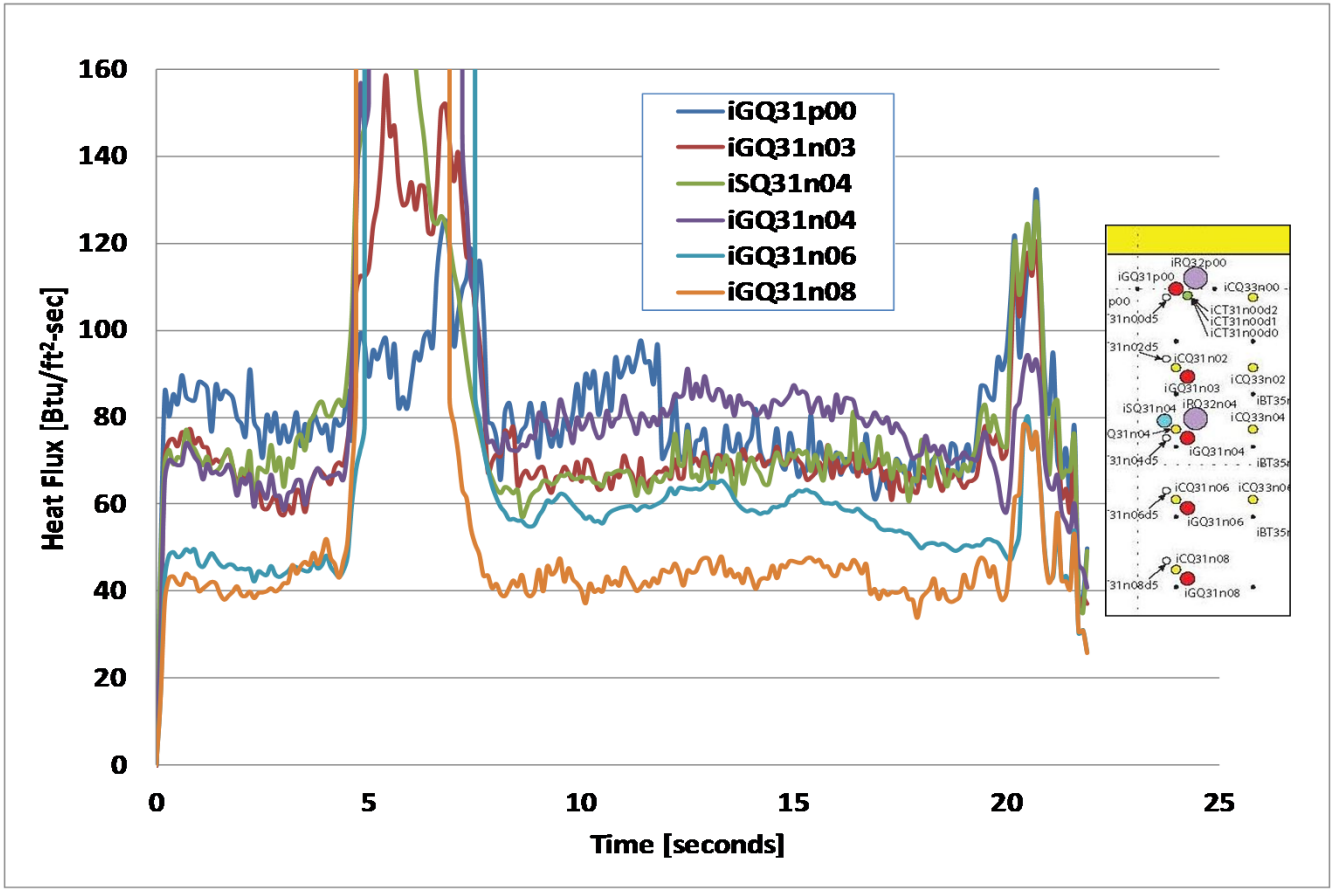

Initial plume heating indicates plume centerline coincident with panel centerline. Spanwise roll-off was about 50% in just 8 inches. Mid-test profiles suggest that the plume may have shifted below the centerline.

Schmidt-Boelter vs. Gardon Gauge
(station 31)

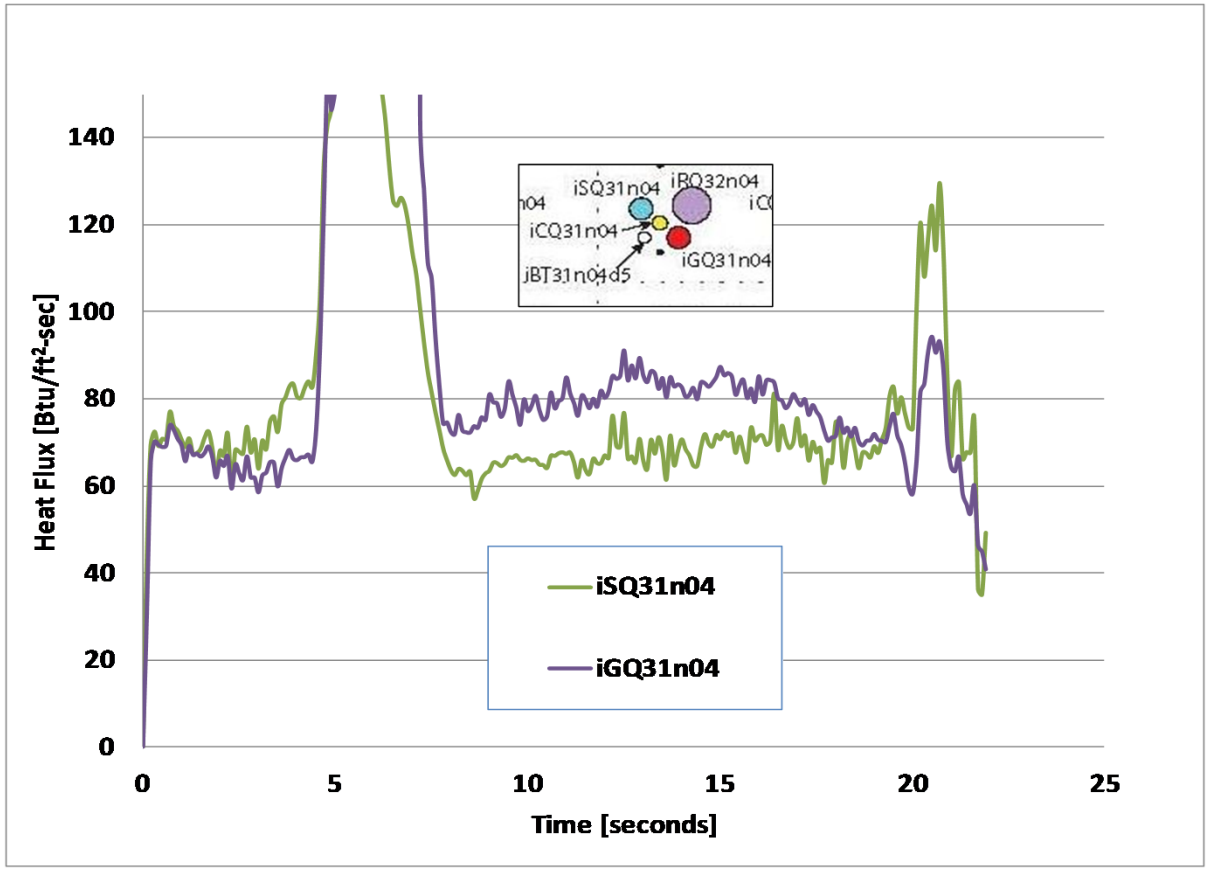

Station 31n04 Schmidt-Boelter and Gardon Gauges initial readings matched well. After the transient event, the readings departed for the remainder of the test.

Conduction Heat Flux via Tri-coaxial Thermocouples
(station 31)

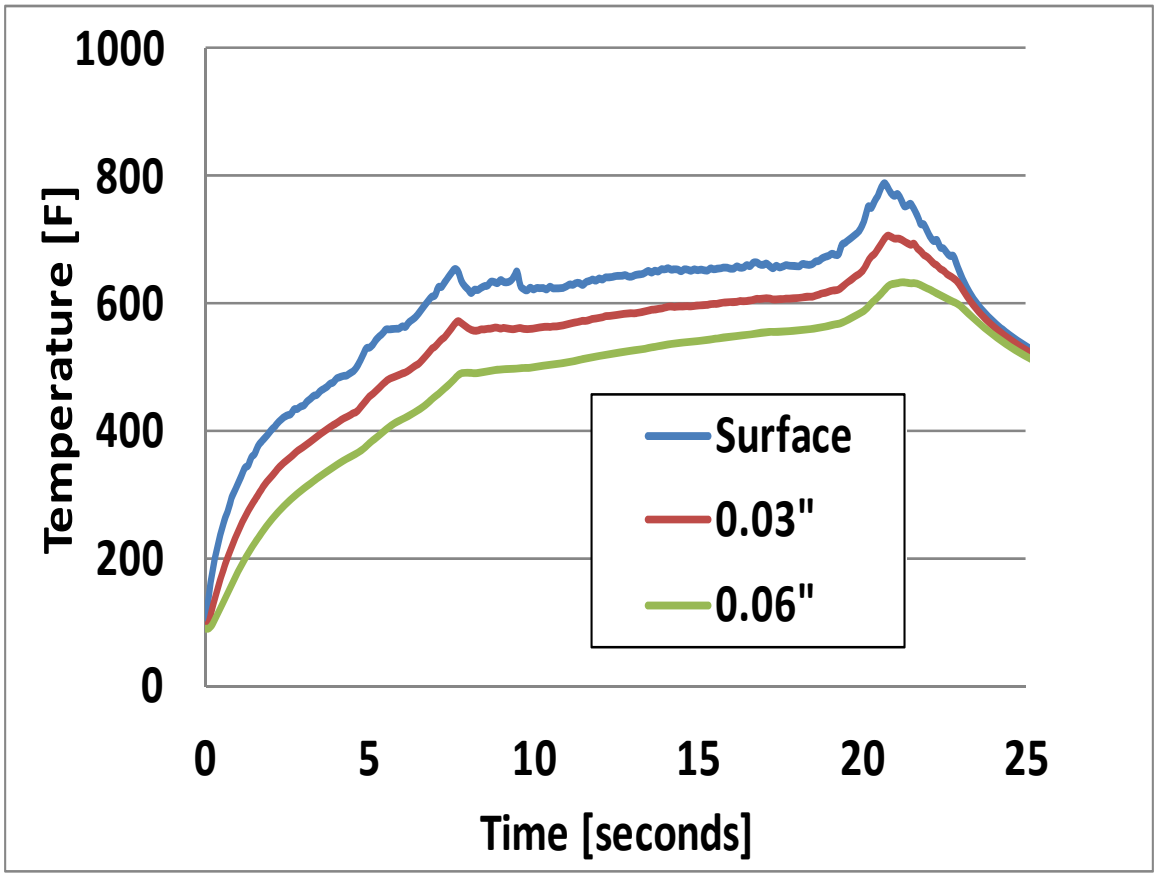

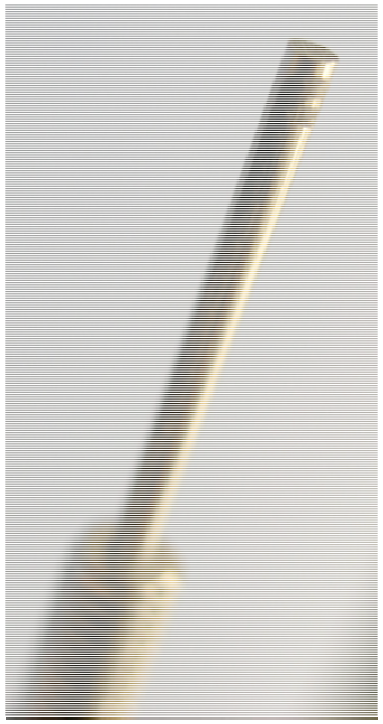

Tri-coaxial thermocouples measured material temperature at three different depths (0, 30, & 60 mils) and indicated that a well behaved thermal gradient was established through the material. Similar trends were observed at axial stations 26 and 35.

Heat Flux via Tri-coaxial Thermocouples
(station 31)

Time [sec]	Surface [F]	0.030" [F]	0.060" [F]	Δz_1 [F]	Δz_2 [F]	Δz_T [F]
1.0	315.0	239.0	178.9	76.1	60.1	136.2
1.1	327.9	250.8	188.8	77.1	62.1	139.1
1.2	339.4	261.6	198.3	77.8	63.3	141.1
1.3	343.1	271.4	207.4	71.6	64.0	135.6
1.4	356.5	279.4	215.7	77.1	63.7	140.8
1.5	363.3	288.6	223.7	74.7	64.9	139.7
1.6	372.4	296.5	231.3	75.9	65.2	141.0
1.7	380.2	305.3	238.9	74.9	66.4	141.3
1.8	387.5	313.1	246.2	74.5	66.9	141.3
1.9	392.2	320.2	253.3	72.0	66.9	138.9
2.0	397.5	326.1	259.7	71.4	66.4	137.8
2.1	402.1	332.1	265.7	70.0	66.4	136.3
2.2	413.6	338.2	271.6	75.5	66.5	142.0
2.3	415.0	344.3	277.6	70.7	66.7	137.4
2.4	418.2	349.0	283.1	69.1	66.0	135.1
2.5	420.8	353.6	288.1	67.2	65.5	132.7
2.6	427.8	357.6	292.7	70.1	64.9	135.1
2.7	430.2	362.2	297.3	68.0	64.9	132.9
2.8	436.7	366.9	301.9	69.8	65.0	134.8
2.9	436.5	370.7	306.3	65.8	64.4	130.2
3.0	442.7	373.9	310.2	68.7	63.7	132.5

ΔT	[R]	72.3	64.9	137.2
Δz	[ft]	0.0025	0.0025	0.0050
k	[Btu/sec-ft-R]	0.00290	0.00290	0.00290
q	[Btu/ft^2-sec]	83.8	75.3	79.6

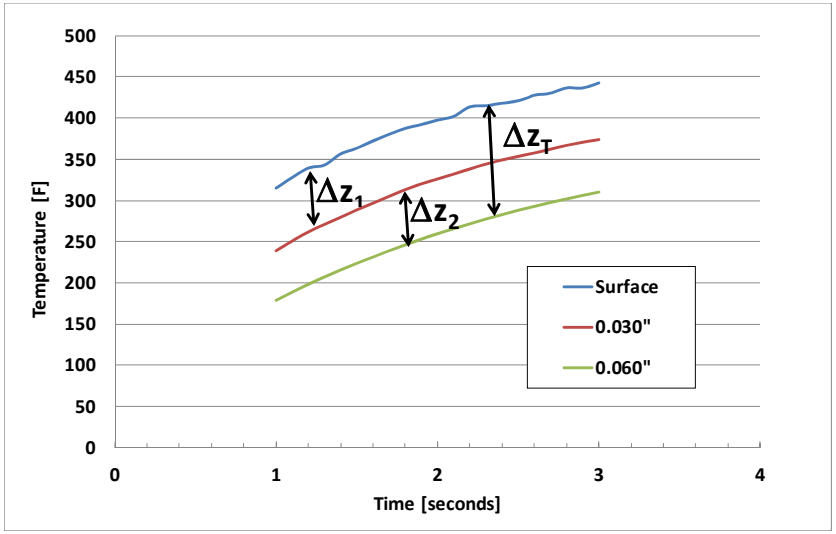

Three separate conduction heat flux measurements are possible with the Tri-coaxial Thermocouple. Thermocouple bead placement is critical for an accurate measurement.

Summary - Heat Flux via Semi-Infinite Analytical Method
(Btu/ft^2-sec)

Type	X	Y	PID NAME	1-3 sec	3-5 sec	5-7 sec	7-9 sec	9-11 sec	11-13 sec	13-15 sec	15-17 sec	17-19 sec	19-21 sec
Coaxial Thermocouple	17	4	iCQ17p04	28.0	26.1	27.2	30.1	24.1	21.9	21.6	20.9	20.8	47.1
Coaxial Thermocouple		-0.5	iCQ17n01	33.7	40.5	55.0	36.7	29.3	27.9	27.4	26.7	24.9	50.0
Coaxial Thermocouple		-4	iCQ17n04	30.7	46.9	79.6	28.2	25.4	26.3	25.8	24.8	22.1	44.0
Coaxial Thermocouple	19	2.25	iCQ19p02	35.4	35.8	41.2	42.1	35.0	32.9	32.1	30.6	29.0	55.6
Coaxial Thermocouple		-2.25	iCQ19n02	36.6	50.3	77.5	36.8	31.0	31.0	30.4	29.5	27.3	52.0
Coaxial Thermocouple		-6	iCQ19n06	29.5	52.3	114.4	30.4	28.8	29.8	28.4	27.6	23.4	43.9
Coaxial Thermocouple	21	1.25	iCQ21p02	39.7	42.7	51.7	47.2	38.8	36.5	35.4	33.7	31.4	54.1
Coaxial Thermocouple		0.75	iCQ21p01	39.6	44.0	54.5	47.1	39.2	37.5	36.2	34.9	32.6	56.3
Coaxial Thermocouple		0.25	iCQ21p01	39.3	45.8	58.5	46.3	37.9	36.3	35.2	34.2	31.6	54.9
Coaxial Thermocouple		-0.25	iCQ21n00	38.9	45.5	58.8	42.4	34.6	32.9	31.7	30.8	28.4	51.3
Coaxial Thermocouple		-0.75	iCQ21n01	41.4	51.4	69.2	44.5	36.8	35.6	34.8	33.9	31.6	55.7
Coaxial Thermocouple		-1.25	iCQ21n02	42.6	53.8	76.3	43.4	35.8	34.9	34.1	33.2	30.7	55.6
Coaxial Thermocouple	23.5	0	iCQ24p00	54.1	58.1	66.8	53.3	45.0	43.1	41.5	40.6	38.0	62.8
Coaxial Thermocouple		-2.25	iCQ24n02	45.5	61.7	108.3	54.4	42.4	41.6	34.6	33.9	31.8	55.6
Coaxial Thermocouple		-4	iCQ24n04	41.7	67.1	155.5	53.7	45.4	45.6	42.6	38.6	33.1	53.8
Coaxial Thermocouple		-6	iCQ24n06	34.4	57.6		44.6	38.5	38.5	36.6	29.4	25.8	42.7
Coaxial Tri-Thermocouple	26	-0.2	iCT26n00d0	66.7	66.5	73.4	57.6	46.1	45.1	43.4	42.2	39.4	67.7
Coaxial Thermocouple		-2.25	iCQ26n02	49.3	61.7	130.7	56.9	48.6	47.3	41.6	39.3	36.8	59.4
Coaxial Thermocouple		-4	iCQ26n04	49.0	72.2		61.5	41.9	42.6	42.5	40.4	36.6	55.5
Coaxial Thermocouple		-6	iCQ26n06	39.3	68.4		55.7	34.9	36.8	36.3	35.0	30.3	45.7
Coaxial Thermocouple	28.5	0	iCQ29p00	72.7	73.4	81.5	83.6	62.2	58.0	56.6	51.1	48.7	79.1
Coaxial Thermocouple		-2.25	iCQ29n02	58.6	71.6	136.3	76.6	54.3	53.6	55.1			
Coaxial Thermocouple		-4	iCQ29n04	53.4	78.1		80.8	47.7	50.1	50.1	48.8	43.9	63.6
Coaxial Thermocouple		-6	iCQ29n06	45.2	76.3		50.4	22.8	32.6	37.3	38.3	29.8	43.9
Coaxial Tri-Thermocouple	31	-0.2	iCT31n00d0	86.8	79.1	85.2	76.2	57.2	55.7	52.4	47.9	46.0	75.6
Coaxial Thermocouple		-2.25	iCQ31n02	68.1	81.5		90.3	67.4	68.7	67.3	60.5	55.8	68.1
Coaxial Thermocouple		-4	iCQ31n04	58.5			82.1	57.7	54.5	51.8	47.5	38.4	42.9
Coaxial Thermocouple		-6	iCQ31n06	51.4	77.9		71.3	44.7	45.8	45.5	44.7	39.5	53.0
Coaxial Thermocouple		-8	iCQ31n08	41.5	68.4		44.2	45.2	45.9	36.8	34.5	29.1	42.3
Coaxial Thermocouple	33	-0.25	iCQ33n00	81.5	76.7	93.0	87.5	63.7	67.4	60.1	60.7	59.6	85.9
Coaxial Thermocouple		-2.25	iCQ33n02	73.7	86.0			91.2	84.0	80.3	73.4	69.6	81.3
Coaxial Thermocouple		-4	iCQ33n04	64.5	91.9								
Coaxial Thermocouple		-6	iCQ33n06	54.7									
Coaxial Tri-Thermocouple	35	-0.2	iCT35n00d0	97.4	86.4			104.2	62.8	65.0	88.0	73.9	86.1
Coaxial Thermocouple		-2.25	iCQ35n02	73.0	87.3		79.6	50.3	52.7	59.2	56.0	63.9	81.2
Coaxial Thermocouple		-4	iCQ35n04	63.5	92.3		103.3	82.6	82.4	78.3	72.7	69.1	
Coaxial Thermocouple		-6	iCQ35n06	60.4			86.3	61.1					
Coaxial Thermocouple		-8	iCQ35n08	50.7	77.9		57.9	46.9	53.5	54.4	54.2	47.7	59.1

-- denotes an over-ranged value

Summary of Spanwise Heat Flux

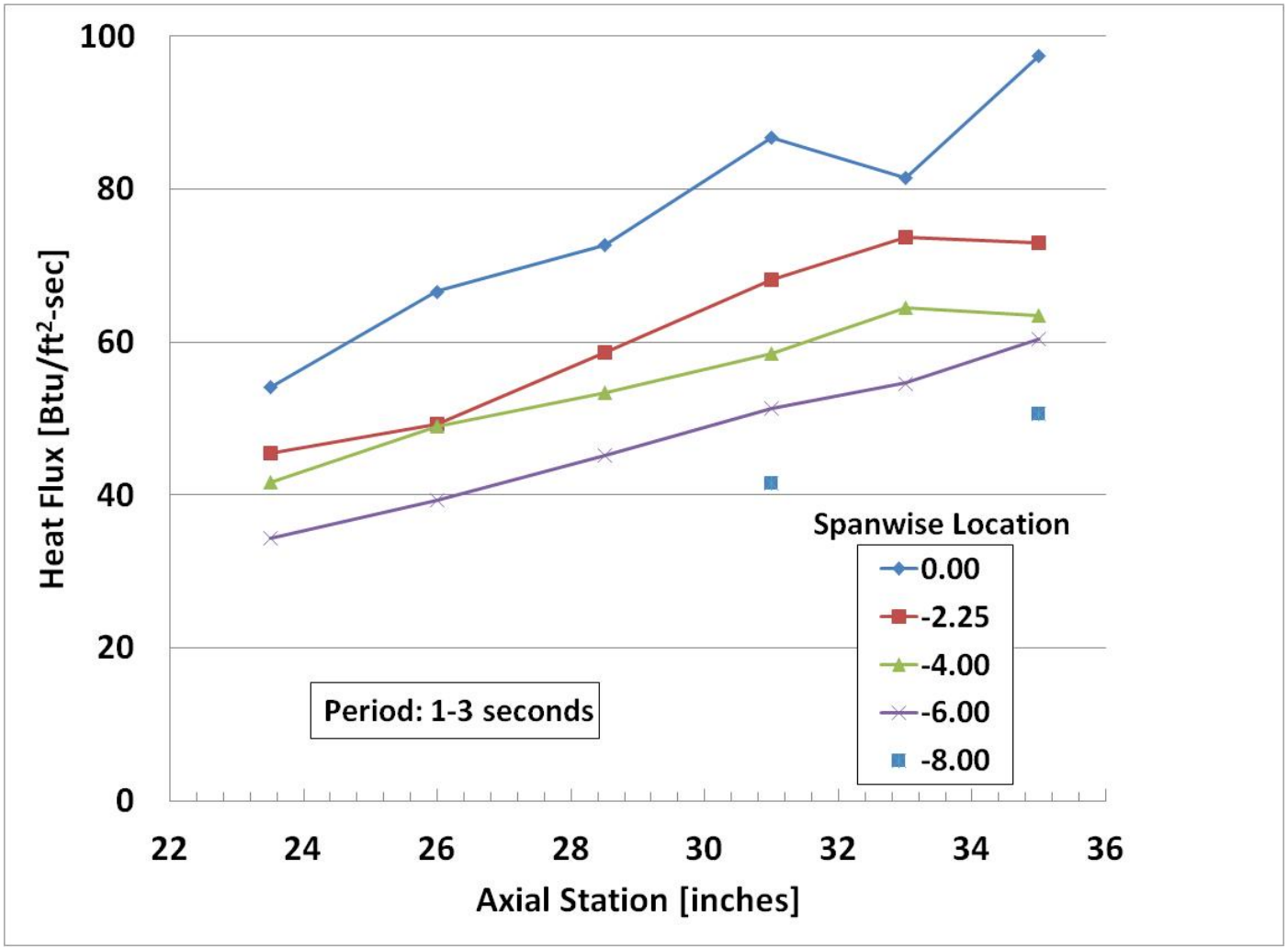

Spanwise heat flux profiles show a consistent heating roll-off trend.

Radiometers
(stations 2, 17, 32)

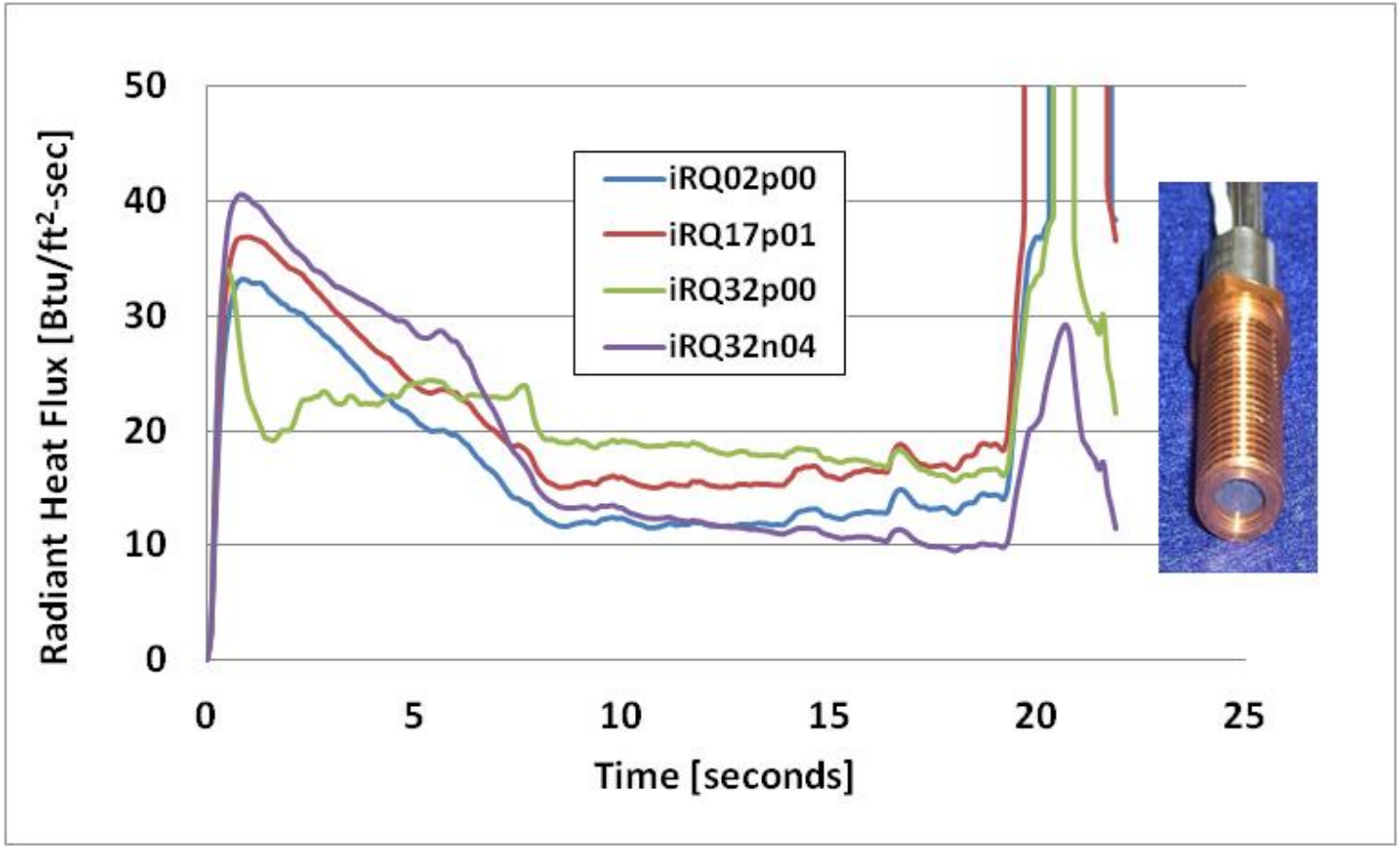

Radiometers over-ranged at both the start and the end of the test (design limit was 30 Btu/ft^2-sec).

Radiant Heating Contribution to Total Heat Flux
(station 17)

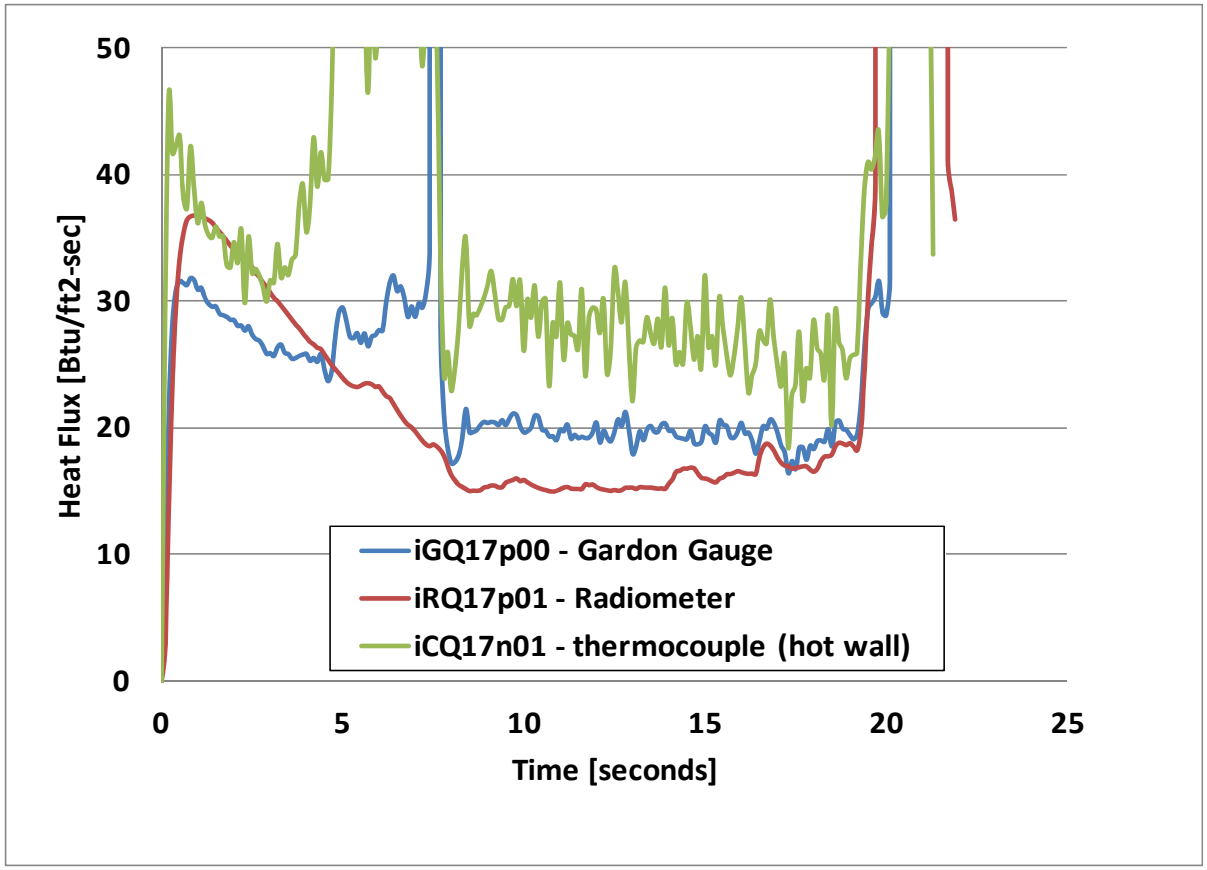

Heat flux via Gardon gauge and Radiometer are in near agreement suggesting that radiant heating at this location accounts for the majority of the total heating. Thermocouple output initially maps to the heat flux gauges but is significantly higher after the transient event.

Radiant Heating Contribution to Total Heat Flux
(stations 31-32)

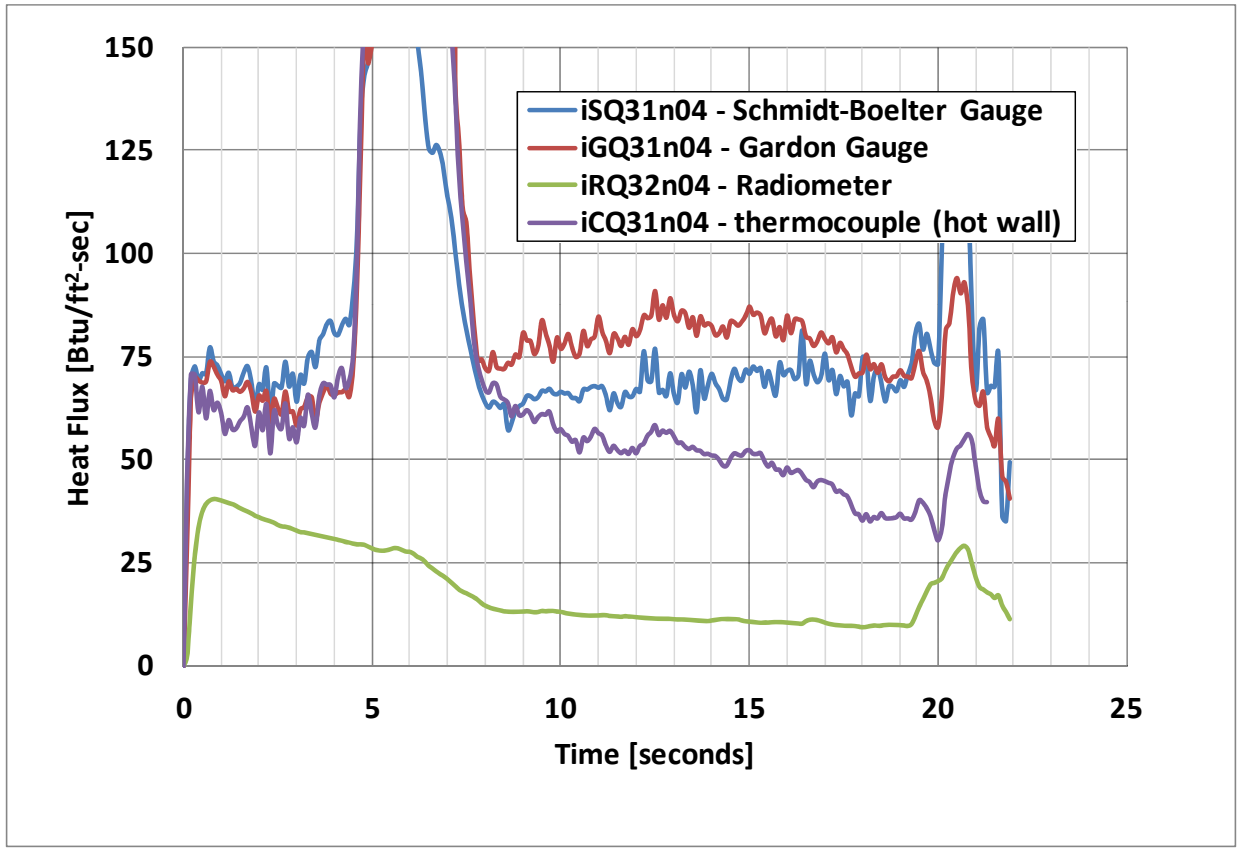

Heat flux gauges and thermocouple are in relative agreement at the start of the test. After the transient event, the Gardon gauge reads significantly higher than the Schmidt-Boelter gauge and the thermocouple departs due to the rise in plate temperature. Radiometer output suggests that radiant heating at this location is about 15% of the total heating.

Centerline Heat Flux Comparisons (all methods)
(stations 9 - 35 for time slice 1-3 seconds)

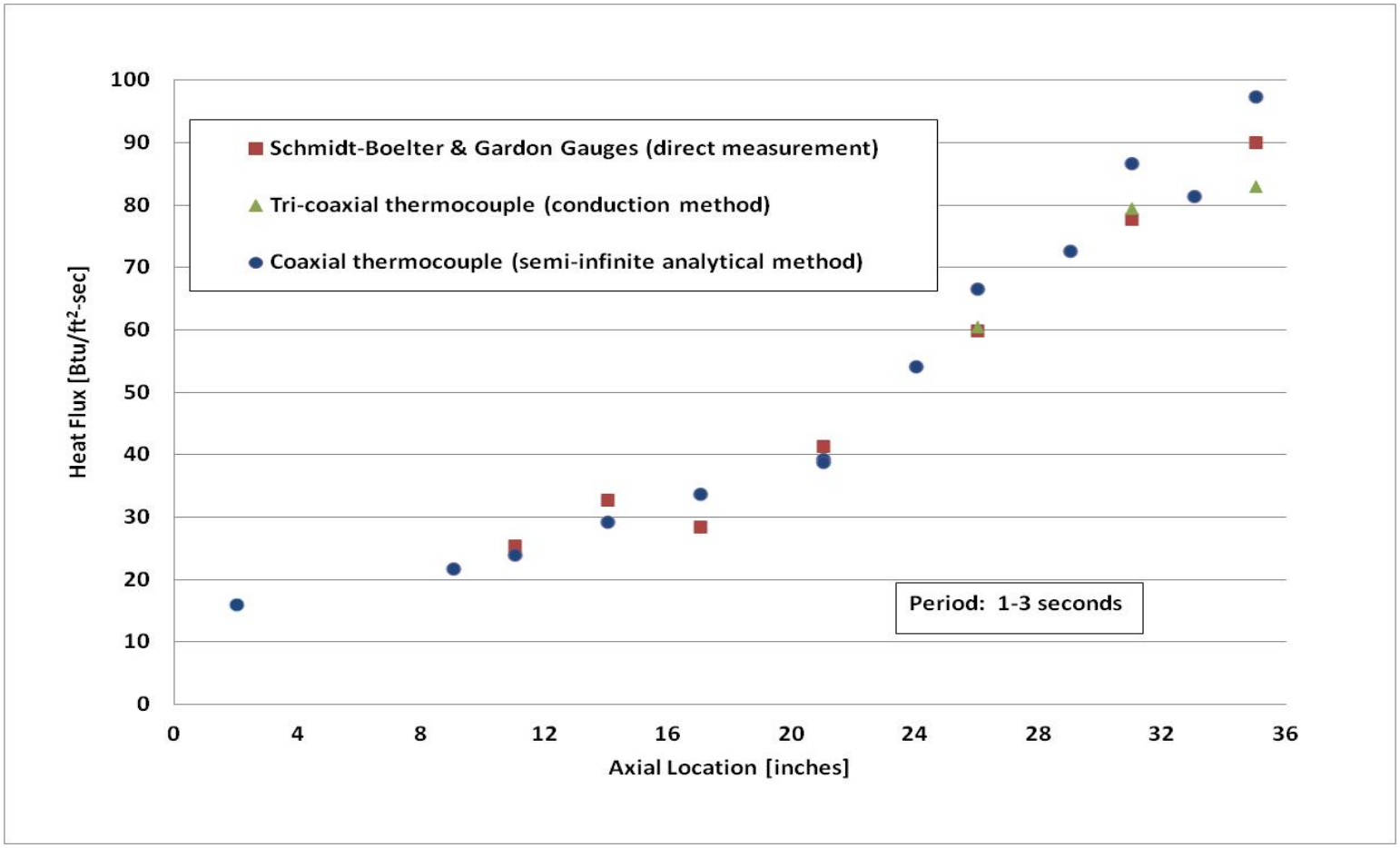

Good agreement was achieved among the three methods. Variances among axial locations varied from 4-12%.

Key Data Observations (Plume)

- **Thermocouple arrays, the heat flux array, and post-test inspection of the panel (which noted aluminum deposition and a non-symmetric burn pattern) indicated that the plume centerline was an inch or more below the panel centerline at some point during the motor test.**

- **Thermal measurements suggest that the motor plume was deflected downward and upstream during the transient event.**

- **Particle plume impingement was not expected to occur on the test article.**
  - **Heat flux measurements were consistent with loads dominated by convective and radiative heating.**
  - ***Yet*, aluminum deposition was observed between stations 30 to 36.**
  - **This deposition affected the data output of several of the thermocouples.**

Key Data Observations (Heating)

- Inspection of the data record suggests that the best time frame for comparison of CFD to test data is prior to the transient event. Most analytical work herein focused on the 1-3 second time slice. This time period showed good agreement among the three heat flux methods.

- There was a greater departure in results from the three heat flux methods at a later time slice (12-14 seconds) as the semi-infinite analytical method may have been affected with thermal buildup from prolonged exposure to a varying heating profile.
  - The coaxial thermocouple indirect surface heat flux method works best for short duration, steady-state thermal loads.
  - For aerothermal testing with long duration, time varying thermal loads use of direct surface heat flux methods (Gardon and Schmidt-Boelter gauges) work best.

- The measured radiative heating was higher than expected and appeared to dominate the forward portion of the test panel.

- Nearly all instrumentation survived the test. All heat flux gauges and radiometers have been recalibrated for reuse and the nine failed coaxial thermocouple junctions were easily reestablished.

Questions?

BACKUP SLIDES

Impact of SRTMV-N2 Plume Impingement Panel Test

LAS Risk Mitigation Project (NESC)

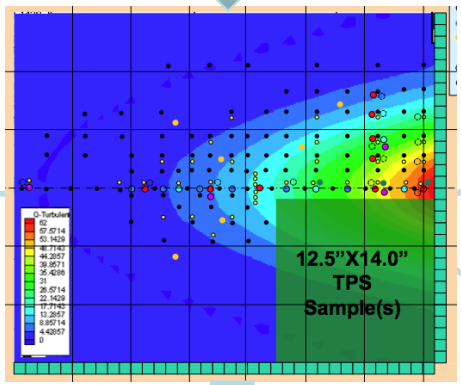

Unique Plume Impingement Database (public)

Commercial Crew Partner Benefits

TPS Risk Mitigation for MPCV (recession rates)

Abort Motor Environment Characterization

Validation Data for Multiple CFD Codes

USM3D | LOCI-CHEM | DPLR | Analytical Methods | …

Instrument Naming Convention

Instrument Type	
BT	Backside Thermocouple
CQ	Coaxial Thermocouple
CT	Tri-coaxial Thermocouple
GQ	Gardon Heat Flux Gauge
RQ	Radiometer
SQ	Schmidt-Boelter Heat Flux Gauge

Thermal Instrument Naming Convention (example: iGQ31n04)	
i	Panel Test Instrument
GQ	Instrument Type (Gardon Gauge)
31	approximate downstream distance from the panel leading edge (inches)
n	centerline orientation n = below the centerline p = above the centerline
04	approximate spanwise distance from the panel centerline (inches)

Tri-coaxial Thermocouple Naming Convention (example: iCT35n00d2)	
i	Panel Test Instrument
CT	Tri-coaxial Thermocouple
35	approximate downstream distance from the panel leading edge (inches)
n	n = below the centerline p = above the centerline
00	approximate spanwise distance from the panel centerline (inches)
d2	d0 = surface measurement d1 = 0.030" below the surface d2 = 0.060" below the surface

Panel Back Wall Temperatures

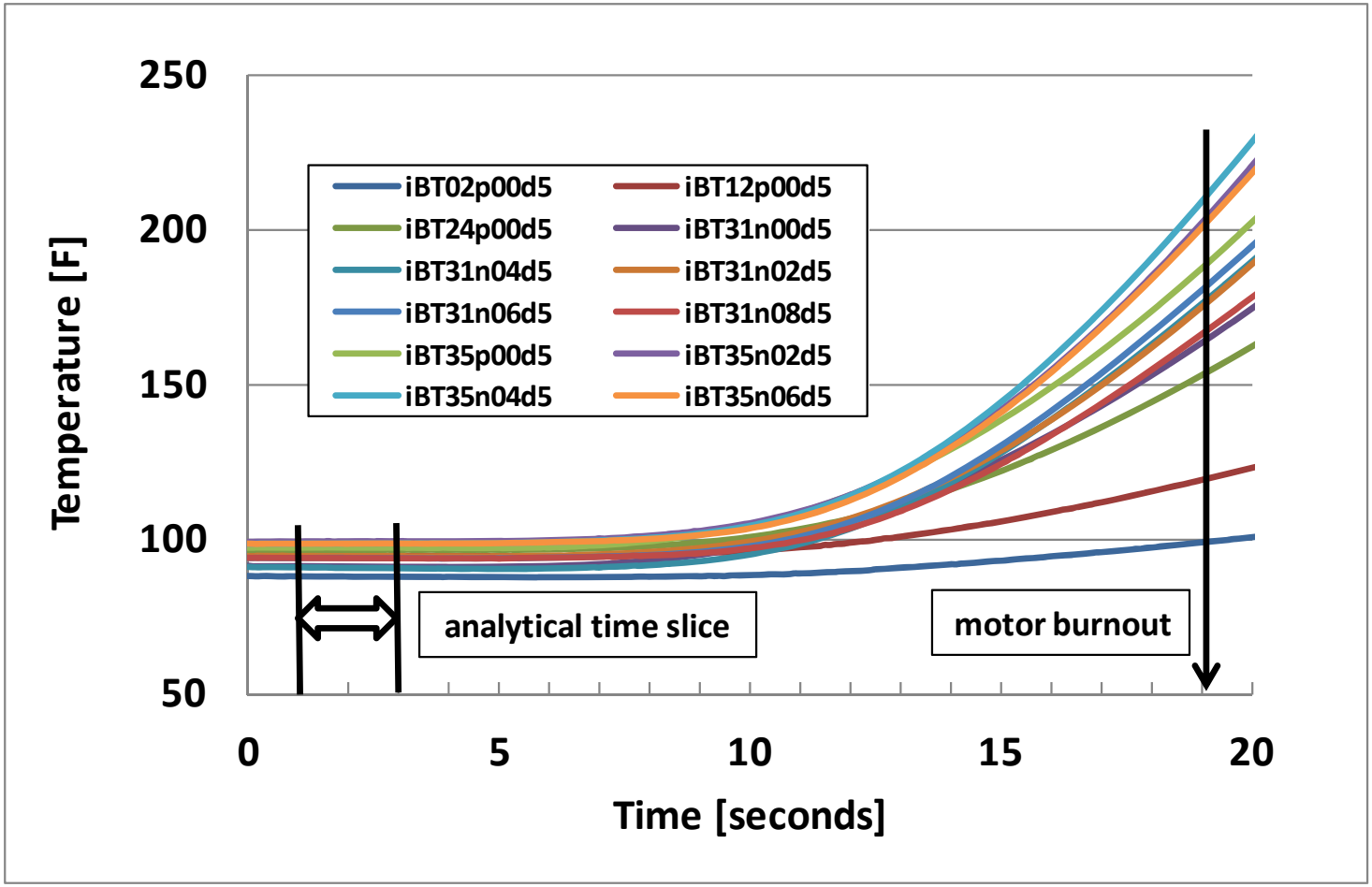

The test plate was 1” thick. Back wall temperatures measurements did not rise appreciably until near the end of the motor burn.

Corrections for the Heat Flux Gauges

- The Schmidt-Boelter and Gardon gauges were water cooled which had the effect of producing a cold wall heat flux measurement.

- To compare these measurements to the semi-infinite analytical method, the convective component of the heat flux gauge readings were adjusted to a hot wall measurement.

- This adjustment was achieved through the following relation:

$$Q_{corrected} = Q_{measured} \bullet \frac{T_{recovery} - T_{measured}}{T_{recovery} - T_{initial}}$$

- As part of this calculation, the recovery temperature of the plume was estimated at 5300 F.

- Since the wall temperature never reached above 1000 F, any correction to the radiative component of the total heat flux gauge would have been negligible.

Centerline Heat Flux Comparisons (all methods) (stations 9 – 35 for time slice 12-14 seconds)

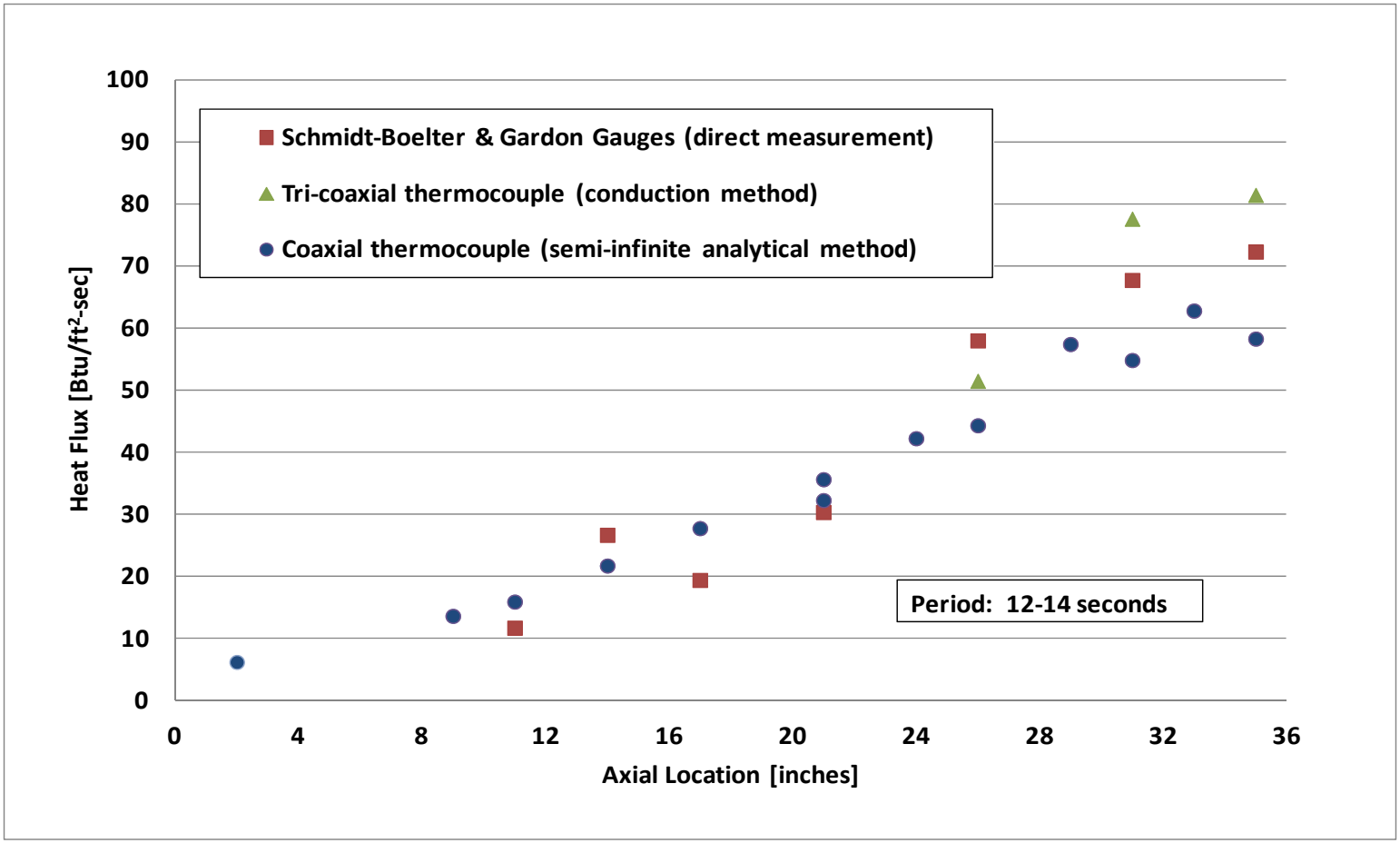

An evaluation of the three heat flux methods at a later time slice showed variances among axial locations from 4-25%. The greatest departure from the earlier time slice appears to be from the semi-infinite analytical method.

Semi-Infinite Analytical Method

- **Approach**
  - **An established method for inferring heat-transfer rates from flows using surface coaxial thermocouple measurements was used in this study. (see Cook, W. J and Felderman, E. J., "Reduction of Data from Thin Film Heat Transfer Gages: A concise Numerical Technique," AIAA Journal, Vol. 4, No. 3, 1966, pp. 561-562.)**
  - **the thermal product of the thermocouple, β, was adjusted as it increased with increasing temperature**
  - **The thermocouple and test plate were thermally matched (similar β=β(T))**
  - **Accuracy increases with the number of terms used. 20 terms yields about a 0.1% variance from an exact solution (Cook, et.al.)**

- **Requirement for the use of this analytical method**
  - **the medium must be treated as a semi-infinite solid**
  - **this assumption was valid for the chosen time slice**

$$\dot{q}(t_n) = \dot{q}_n = \frac{2\beta}{\sqrt{\pi}} \sum_{i=1}^{i=n} \frac{T_i - T_{i-1}}{\sqrt{t_n - t_i} + \sqrt{t_n - t_{i-1}}}$$

$$\beta = \sqrt{\rho c k}$$

TIME DEPENDENT HEAT FLUX PROFILE

Time [sec]	Temperature [F]	Temperature [R]	Heat Flux [Btu/ft2-s]	Heat Flux [Watts/m2]
0.000	540.000	999.670	----------	
0.100	547.700	1007.370	0.1078E+01	0.1224E+05
0.200	551.500	1011.170	0.9781E+00	0.1111E+05
0.300	554.400	1014.070	0.9686E+00	0.1100E+05
0.400	556.800	1016.470	0.9617E+00	0.1092E+05
0.500	558.900	1018.570	0.9589E+00	0.1089E+05
0.600	560.900	1020.570	0.9726E+00	0.1105E+05
0.700	562.600	1022.270	0.9580E+00	0.1088E+05
0.800	564.300	1023.970	0.9713E+00	0.1103E+05
0.900	565.900	1025.570	0.9758E+00	0.1108E+05
1.000	567.300	1026.970	0.9630E+00	0.1094E+05
1.100	568.700	1028.370	0.9692E+00	0.1101E+05
1.200	570.100	1029.770	0.9794E+00	0.1112E+05
1.300	571.400	1031.070	0.9777E+00	0.1110E+05
2.200	581.200	1040.870	0.9698E+00	0.1101E+05
2.300	[illegible]	[illegible]	0.9824E+00	0.1116E+05
2.400	[illegible]	[illegible]	[illegible]749E+00	0.1107E+05
2.500	[illegible]	[illegible]	[illegible]897E+00	0.1124E+05
2.600	[illegible]	[illegible]	[illegible]838E+00	0.1117E+05
2.700	585.800	1045.470	0.9717E+00	0.1103E+05
2.800	586.700	1046.370	0.9830E+00	0.1116E+05
2.900	587.600	1047.270	0.9882E+00	0.1122E+05
3.000	588.400	1048.070	0.9793E+00	0.1112E+05
3.100	589.200	1048.870	0.9788E+00	0.1112E+05
3.200	590.000	1049.670	0.9797E+00	0.1113E+05
3.300	590.800	1050.470	0.9815E+00	0.1115E+05
3.400	591.600	1051.270	0.9839E+00	0.1117E+05
3.500	592.400	1052.070	0.9867E+00	0.1121E+05
3.600	593.200	1052.870	0.9899E+00	0.1124E+05
3.700	593.900	1053.570	0.9793E+00	0.1112E+05
3.800	594.700	1054.370	0.9912E+00	0.1126E+05
3.900	595.400	1055.070	0.9824E+00	0.1116E+05
4.000	596.100	1055.770	0.9814E+00	0.1115E+05
4.100	596.800	1056.470	0.9816E+00	0.1115E+05
4.200	597.500	1057.170	0.9824E+00	0.1116E+05
4.300	598.200	1057.870	0.9838E+00	0.1117E+05
4.400	598.900	1058.570	0.9855E+00	0.1119E+05
4.500	599.600	1059.270	0.9875E+00	0.1121E+05
4.600	600.300	1059.970	0.9897E+00	0.1124E+05
4.700	600.900	1060.570	0.9781E+00	0.1111E+05
4.800	601.600	1061.270	0.9889E+00	0.1123E+05
4.900	602.300	1061.970	0.9930E+00	0.1128E+05
5.000	602.900	1062.570	0.9825E+00	0.1116E+05

Summary – Total and Radiative Heat Flux (Cold Wall)

Total Heat Flux Gauges (Btu/ft^2-sec)

Sensor	FS	1-3 sec	3-5 sec	5-7 sec	7-9 sec	9-11 sec	11-13 sec	13-15 sec	15-17 sec	17-19 sec	19-21 sec
iGQ11p00	20	25.4	23.8	25.6	16.7	12.7	11.7	11.9	12.3	12.3	
iSQ14p00	20					29.1	27.4	27.4	27.8	27.0	
iGQ17p00	20	28.4	26.0	28.7		20.2	19.6	19.4	19.7	18.8	
iGQ21p00	50	41.8	42.8	46.5	37.2	31.9	31.9	31.2	31.4	29.8	53.2
iSQ26p00	100	61.8	64.8	80.2	71.4	62.3	63.5	61.1	57.8	54.8	90.2
iGQ31p00	250	81.4	80.7	97.7	88.9	82.8	82.1	72.7	69.2	68.0	94.4
iGQ31n03	100	66.3	74.7	134.9	87.3	66.8	68.2	70.1	68.8	65.9	86.0
iSQ31n04	100	68.3	93.3		73.8	65.9	67.1	68.0	71.1	68.5	90.6
iGQ31n04	100	64.9	81.6			78.8	82.7	83.3	82.2	73.7	75.0
iGQ31n06	50	45.2				58.7	61.5	60.8	59.7	51.7	55.5
iGQ31n08	50	40.0			47.9	42.4	43.8	44.4	45.0	39.1	52.5
iGQ35p00	500	94.8	87.6	106.9	97.4	82.3	80.7	83.2	88.4	75.2	92.3

Radiometers (Btu/ft^2-sec)

Sensor	FS	1-3 sec	3-5 sec	5-7 sec	7-9 sec	9-11 sec	11-13 sec	13-15 sec	15-17 sec	17-19 sec	19-21 sec
iRQ02p00	20		24.1	18.9	13.1	11.97	11.78	12.31	13.14	13.55	
iRQ17p01	20		27.3	22.4	16.9	15.44	15.23	15.85	16.79	17.51	
iRQ32p00	20	21.4	22.8	23.5	20.9	18.79	18.42	17.94	17.38	16.27	
iRQ32n04	20			26.3	15.8	12.94	11.91	11.26	10.76	9.947	

-- denotes an over-ranged value